Social-like responses are inducible in asocial Mexican cavefish despite the exhibition of strong repetitive behaviour.

Motoko Iwashita and Masato Yoshizawa

School of Life Sciences, the University of Hawai‘i at Mānoa, Honolulu, Hawai‘i, USA

Corresponding:

Masato Yoshizawa

2538 McCarthy Mall, EDM 216, Honolulu, HI 96822

yoshizaw@hawaii.edu

Abstract

Social behaviour is a hallmark of complex animal systems; however, some species appear to have secondarily lost this social ability. In these non-social species, whether social abilities are permanently lost or suppressed is unclear. The blind cavefish *Astyanax mexicanus* is known to be asocial. Here, we reveal that cavefish exhibited social-like interactions in familiar environments but suppressed these interactions in stress-associated unfamiliar environments. Furthermore, the level of suppression in sociality was positively correlated with that of stereotypic repetitive behaviour, as seen in mammals. Treatment with a human antipsychotic drug targeting the dopaminergic system induced social-like interactions in cavefish, even in unfamiliar environments, while reducing repetitive behaviour. Overall, these results suggest that the antagonistic relationship between repetitive and social-like behaviours is deeply shared from teleosts through mammals.

Main text

Introduction

Many animals across a wide range of taxa express collective behaviours (e.g., shoaling and herding) resulting in multiple benefits, including foraging and/or antipredator effects (Pitcher and Parrish, 1993). Despite the benefits of collective behaviour, this type of behaviour in some species has been reduced over evolutionary time such that these species exhibit marked asociality when compared to their socially closest relatives (Pitcher and Parrish, 1993). Additionally, even among social species, this collective behaviour can disappear when the animal is exposed to a stress-associated environment (Kim et al., 2016; Lewis et al., 2007). Instead, these animals may express asocial behaviour and/or stereotypic repetitive behaviours, which have been particularly well characterized in mammals (*e.g.*, "zoochosis") (Lewis et al., 2007; Rose et al., 2017). Stereotypic repetitive behaviours, in contrast to collective behaviours, are generally thought of as non-functional (Lewis et al., 2007). Psychiatric conditions in humans, such as autism spectrum disorder (ASD), share similarities to atypical repetitive behavioural responses in other animals in that social activity is decreased and there is an overall increase in stereotypic repetitive behaviours, especially in stress-inducing environments (Kaplan and McCracken, 2012; Langen et al., 2011a; Runco et al., 1986). The neural mechanisms underlying the contrasting expression of social and repetitive behaviours and how the 'choice' between stereotypic repetitive and social modes of behaviour are made remain largely unknown (Kazdoba et al., 2016; Kim et al., 2016; Langen et al., 2011b; Lewis et al., 2007). However, studies in mammals have hinted at such neural mechanisms by indicating that the dopaminergic striatal system is key for behavioural choices. For example, treatment with anti-agitation drugs (i.e., drugs to reduce repetitive behaviour, e.g., aripiprazole and risperidone) attenuated but did not

49 eliminate the activity of the D2-dopamine receptor-based indirect pathway in mammals (Grillner,
50 2018; Kim et al., 2016). Importantly, this core dopaminergic system exists in all vertebrate
51 models from lampreys, teleosts (zebrafish), amphibians (Xenopus), and birds (chickens) to
52 mammals (mice and humans) (Grillner and Robertson, 2016; Stephenson-Jones et al., 2011).
53 However, among actinopterygians (ray-fin vertebrates), it is largely unknown whether an
54 evolved asocial population had lost the ability to congregate with each other or just suppressed
55 this activity and whether repetitive behaviours are enhanced under stress in an antagonistic
56 manner with collective behaviour.

57 To address these two questions, we used a suitable vertebrate model, the Mexican tetra
58 *Astyanax mexicanus*, and developed a novel experimental workflow to assay collective and
59 stereotyped behaviour (Yoshizawa, 2015). *A. mexicanus* is emerging as a key model system for
60 the study of diverse aspects of evolution and development, including those with relevance to
61 human medicine, e.g., cataract formation, obesity, diabetes, albinism-related syndrome, and
62 insomnia (Aspiras et al., 2015; Bilandžija et al., 2018, 2013; Duboué et al., 2012, 2011; Jaggard
63 et al., 2017; Keene et al., 2016; Ma et al., 2014; McGaugh et al., 2014; Riddle et al., 2018;
64 Rohner et al., 2013; Strickler et al., 2007). *A. mexicanus* comprises surface riverine epigean
65 (surface fish) and cave-dwelling hypogean (cavefish) forms. Cavefish diverged from their
66 surface-dwelling relatives 20,000~200,000 years ago (Fumey et al., 2018; Herman et al., 2018)
67 and since then have evolved many distinct morphological and behavioural phenotypes, including
68 eye regression/loss, pigment reduction, increased number of lateral line mechanosensors,
69 enhanced behaviour responses to vibrational stimuli, sleeplessness, hyperactivity and repetitive
70 circling (Keene et al., 2016; Yoshizawa, 2015; Yoshizawa et al., 2018). Compared to cavefish,
71 surface fish show mainstream phenotypes, including eyed and pigmented morphologies, no

strong sensitivity to vibrational stimuli, and nocturnal sleep patterns. Cavefish have also been shown to have reduced social-like interactions, such as no detectable schooling and shoaling behaviour (Kowalko et al., 2013; Patch et al., 2020; Pierre et al., 2020) or hierarchal dominance (Elipot et al., 2013). In contrast, surface fish school/shoal with cohorts and model fish (Kowalko et al., 2013) show group hierarchical dominance (Elipot et al., 2013). Importantly, the surface fish schooling behaviour was concluded to be driven by visual stimuli because it diminished in the dark (Kowalko et al., 2013). In contrast, surface fish in the dark continued to show similar levels of aggression and were thought to establish a hierarchical dominance, similar to those kept in the light (Elipot et al., 2013). This motivated us to test other social-like interactions in the dark to compare non-visual-based social-like interactions between surface fish and cavefish.

Thus, we developed a more sensitive method to detect social-like interactions and repetitive behaviour in the dark (Figure 1). This method revealed a number of social-like interactions in surface fish in the dark. Surface fish, however, did not show repetitive turning. Furthermore, we also revealed weak but existent social-like interactions in cavefish that occurred while exhibiting a significantly higher level of repetitive behaviour than that of surface fish. During these nearby interactions, cavefish decelerated their swimming speed and were likely to follow their cohorts. The comparison of these behaviours under familiar and potentially stressful, unfamiliar environments indicated that cavefish showed significantly more nearby interactions in the familiar environment. The atypical dopamine psychiatric drug aripiprazole, which is known to increase social behaviours and reduce repetitive motions in humans (Coleman et al., 2019; de Bartolomeis et al., 2015; Ghanizadeh et al., 2014), reduced swimming speed and increased nearby interactions in cavefish. Cavefish also showed reduced levels of repetitive turning after aripiprazole treatment. In summary, cavefish showed robust repetitive circling, and the degree of

circling was negatively correlated with social-like nearby interactions. This cavefish interaction remained plastic and was suppressed under a potentially stressful environment. Together with the reported parallels in pharmacological responses, a set of behavioural symptoms, and gene expression profiles between cavefish and humans (Yoshizawa et al., 2018), the presented results suggest that the asocial cave population is still capable of performing social-like nearby interactions under environmental or pharmacological treatments and shares an antagonistic association between social-like and repetitive behaviours with mammals.

Results

Detecting nearby interactions in a non-visual, infrared-illuminated condition

Since there are few reports on social-like interactions of teleost species in the dark (e.g., Gerlai, 2014), we began by systematically assessing close-distance interactions using social and non-social morphs of *Astyanax mexicanus*—surface fish and cavefish—in a non-visual setup. Fish were introduced into an unfamiliar environment, the recording arena, where we could observe nearby interactions at close range (see below). The behaviours of four fish were recorded for 5 min (Figure 1; Videos 1 and 2) in a black box that was evenly back-lighted with an 850-nm light-emitting diode (LED) (Materials and Methods). The individual trajectory of each of the four individual fish was tracked by idTracker (Pérez-Escudero et al., 2014). To verify whether fish visually responded under 850-nm lighting, surface fish and cavefish were tested for phototaxis and startle responses when presented with a moving shade. Neither surface fish nor cavefish showed phototaxis or a preference for illuminated or non-illuminated areas (Figure 1—figure supplement 1). In addition, sighted surface fish did not avoid the shade approaching them (Video 3). These results suggested that neither surface fish nor cavefish visually responded under 850-nm illumination. We call this non-visual setup the 'dark' condition hereafter.

Surface fish are known to school/shoal in lighted environments (Kowalko et al., 2013; Wilkens et al., 1988) and exhibited strong shoaling and schooling in our setup in lighted conditions (Video 4; see below). In the dark, two standard shoaling measurements (Miller et al., 2013; Partridge et al., 1980; Pitcher, 1973)—the averages of nearest neighbour distance (NND: the distance between a focal individual and its nearest neighbour) and inter-individual distance (IID: the mean distance between each individual)—of surface fish were indistinguishable from those of cavefish (Figure 2A and B). However, we observed differences in how cohorts of

126 cavefish and surface fish interacted; in particular, surface fish changed their swimming directions
127 and followed each other, while cavefish showed this pattern less frequently (Figure 2C). Due to
128 the relatively low shoaling tendency of surface fish in the dark and the difficulty of detecting
129 interactions between any two arbitrary fish in IID and NND, a new measurement of this social-
130 like interaction was needed. Here, we define "nearby interaction" as two fish coming within a
131 short distance from each other and then staying close for some period at a level higher than
132 chance. These criteria can suggest intent in the movement rather than random locomotion with
133 respect to their conspecifics. First, to determine the criteria for the maximum distance (cut-off
134 distance) and the minimum duration (cut-off duration) to use in defining a bout of nearby
135 interaction, we employed random sampling by choosing 4 fish among 18 groups (each group
136 consisted of 4 surface fish). These simulated random data enabled us to validate whether fish
137 were closer to each other than by random expectation. A total of 1,280 random samples were
138 performed with the surface fish (see Materials and Methods). By using the X-Y coordinates of
139 randomly sampled surface fish, the IID in each frame was calculated and plotted as a histogram,
140 and this was considered the simulated no-interaction conditions (the blue lines in Figure 2D).
141 The actual surface fish IID scores ranged from 0.0 to 55.0 cm and showed significant differences
142 in event counts between the 3.0- and 6.0-cm cut-offs compared to the simulated surface fish IID
143 scores (Figure 2D). We then selected the second longest distance, 5.0 cm, as a relatively
144 conservative cut-off distance (Figure 2D; Figure 2—figure supplement 1A). Using this cut-off
145 distance, we surveyed the minimum cut-off duration, ranging from 0.0 to 40.0 s (Figure 2E). The
146 minimum cut-off durations ranging from 3.0 to 8.0 s with the actual surface fish data resulted in
147 significantly more nearby-interaction event counts than those of the simulated surface fish data.
148 We thus chose the second shortest duration, 4 s, as a relatively conservative minimum cut-off

149 duration (Figure 2E; Figure 2—figure supplement 1B). With these criteria (≤ 5 cm and ≥ 4 s)
150 defining nearby interactions, we standardized nearby interactions by subtracting passing-by
151 durations (PbDur) calculated from the average swimming speed of each group (Figure 2—figure
152 supplement 1C; Materials and Methods; Supplementary File 2). With these criteria and methods,
153 nearby interactions were detected in both surface fish and cavefish (Figure 2—figure supplement
154 1B, D, and E-G).

155 Next, we evaluated whether these detected interactions were reciprocal rather than
156 unidirectional, as seen in aggression and/or foraging. First, if the detected nearby interactions
157 included aggression/foraging activities, the fish would accelerate towards the target or accelerate
158 to escape (personal observation)(Elipot et al., 2013). To test this possibility of acceleration, shifts
159 in speed were assessed by comparing speeds (i) during a 4-s period directly before the bout of a
160 nearby interaction, (ii) during the bout, (iii) during a 4-s period after the bout, and (iv) during the
161 rest of the recording time. Remarkably, both surface fish and cavefish slowed rather than
162 accelerated during the nearby-interaction bouts compared to before the bouts (Figure 2F;
163 Supplementary File 1). This speed shift from before to during the bout was not detected in the
164 simulated data (Figure 2F; Supplementary File 1). Note that no sign of fin or scale damage was
165 observed after each of the nearby-interaction assays, which has previously been reported in *A.*
166 *mexicanus* in situations involving foraging or aggression against intruders (Elipot et al., 2013).
167 Second, we visualized reciprocal interactions during the nearby interaction by categorizing the
168 patterns of gathering and dispersing into five categories: two fish disperse, two fish swim by in
169 an inverse direction, two fish gather, fish 1 leads, and fish 2 leads (Figure 2—figure supplement
170 2A and B). The raster plots show switches between the leader and follower within each bout in
171 the same pairs (yellow and orange); in the raster plots, we colour-coded these 5 types of

172 interaction categories (Figure 2—figure supplement 2C and E). These switches were observed in
173 both surface fish and cavefish and were also observed in schooling surface fish in the lighted
174 condition (Figure 2—figure supplement 3; Videos 1, 2 and 4). Taken together, we defined
175 nearby interactions as reciprocal social-like interactions, which were observed in both surface
176 fish and cavefish in the dark.

177 Regarding these nearby interactions (shorter than 5.0-cm distance and more than 4.0-s
178 duration), both surface fish and cavefish showed significantly longer durations in these
179 interactions than randomly sampled simulated data (Figure 2G). The actual during-bout speeds in
180 both the surface fish and cavefish were lower than speeds out of the bouts (Figure 2F). Cavefish
181 speed during the bout was also significantly lower than the after-bout speed (right panel: Figure
182 2F). In contrast, in the simulated data, the swimming speed during a bout was indistinguishable
183 from other speeds in cavefish (left panel: Figure 2F) and both before- and after-bout speeds in
184 surface fish (Figure 2F). The surface fish during-bout speed was, however, lower than the out-of-
185 bout speed in the simulated data, which we suggest was due to arena constraints and is discussed
186 later (Figure 2F). These results suggested that not only surface fish but also 'asocial' cavefish
187 can express social-like interactions in the dark at a significantly higher than random chance level.
188

189 <u>Involvement of lateral line mechanosensors in nearby interactions in the dark</u>

190

191 Previous research has strongly suggested that the lateral line is the major sensor
192 controlling shoaling/schooling among non-visual sensory systems (Bleckmann, 1986;
193 Montgomery et al., 2013). To tested the involvement of lateral line mechanosensors, we
194 employed a method of pharmacological ablation of the lateral line by applying gentamicin

195 aminoglycoside antibiotics—an established method for ablating the lateral line sensors of
196 teleosts, including *A. mexicanus* (Figure 2—figure supplement 4) (Yoshizawa et al., 2010).
197 Gentamicin treatment diminished the functional neuromasts—the sensory units of the lateral line
198 labelled by a DASPMI vital dye—in both surface fish and cavefish (Figure 2—figure
199 supplement 4B-E) (Van Trump et al., 2010; Yoshizawa et al., 2010) and reduced the duration of
200 nearby interactions in surface fish ($P = 0.0112$; Figure 2—figure supplement 4A). In contrast,
201 there was no detectable change in nearby interactions in cavefish ($P > 0.05$, Figure 2—figure
202 supplement 4A), although the neuromasts were ablated in a manner similar to surface fish
203 (Figure 2—figure supplement 4B-E). Accordingly, this result suggested that lateral line sensors
204 contributed to social-like interactions in surface fish in the dark.
205
206 <u>Effects of familiar and unfamiliar environments on nearby interactions</u>
207 In mammals, social tendencies are suppressed in novel unfamiliar environments (Boulter
208 et al., 2014; Buhr and Dugas, 2009; Kim et al., 2016). We therefore tested whether a similar
209 behavioural response could be observed in the two *Astyanax* morphs by measuring the level of
210 social-like interactions in response to familiar and unfamiliar environments (Figure 3A).
211 In both the familiar and unfamiliar environments, after their introduction to the recording
212 arena, surface fish dispersed and swam slightly more often in the periphery than in the centre of
213 the arena, which may represent thigmotaxis (Figure 3B, C; the position indices were below 0.5)
214 (Patton et al., 2010). Within one minute after release, surface fish started intermittently following
215 nearby cohorts. Cavefish also dispersed following transfer (Figure 3C) but showed greater
216 swimming distance than surface fish (Figure 3D). Cavefish followed their cohorts less frequently
217 than surface fish (see below). Notably, surface fish had significantly lower swimming distances

218 in the unfamiliar environment than in the familiar environment, but the swimming distance in
219 cavefish was not altered based on the environments (Figure 3D). Implementing the novel metric
220 for nearby interactions, analysis of social-like interactions revealed that surface fish and cavefish
221 responded differently to unfamiliar environmental stimuli (Figure 3F and G; Pop × Env: $P <$
222 0.0004 and $P < 0.0095$, respectively; Supplementary File 1). In surface fish, the unfamiliar
223 environment significantly increased nearby-interaction duration and bout number (Figure 3F and
224 G; $r = 0.388$, $P = 0.0021$ and $r = 0.381$, $P = 0.0025$). In contrast, the unfamiliar environment
225 reduced nearby-interaction durations in cavefish (Figure 3F and G; $r = 0.243$, $P = 0.0397$ and $r =$
226 0.200, $P = 0.09$; Supplementary File 1). Notably, in the familiar environment, the levels of
227 nearby-interaction durations of surface fish and cavefish were comparable, which suggested that
228 social-like nearby interaction is inducible in cavefish.

229 Regarding swimming speed during nearby interactions (Figure 3H), surface fish were
230 more active in the familiar environment than in the unfamiliar environment, as shown in the
231 swimming distance scores (Figure 3D). However, surface fish did not reduce their swimming
232 speed during the bout compared to other time periods (the only exception was the out-of-bout
233 speed in the unfamiliar environment; Figure 3H). Considering the difference from the previous
234 surface fish experiment performed in the unfamiliar environment (actual data in Figure 2F),
235 where surface fish significantly reduced the during-bout speed compared with the before-bout
236 speed, surface fish did not consistently reduce their speed in the nearby interactions, yet speed
237 reductions were occasionally detected.

238 The speed profile of the cavefish did not change between the familiar and unfamiliar
239 environments (speed: $F_{3,198} = 5.7$, $P = 0.0009$; env (fam vs unfam): $F_{1,198} = 0.3$, $P = 0.5655$;
240 speed×env: $F_{3,198} = 0.8$, $P = 0.4825$); however, the swimming velocity of cavefish significantly

241 reduced during the interaction bout, suggesting that they responded to their cohorts, regardless of
242 their familiarity with the environment (Figure 3H; Supplementary File 1). In summary, surface
243 fish and cavefish differentially responded to environmental stimuli, and cavefish expressed a
244 comparable level of nearby interactions to surface fish in a familiar environment.
245
246 Turning bias index as a measure of repetitive circling and its relationship to nearby interactions
247 In mammals, social tendencies seem to be suppressed in those who show stereotypic
248 repetitive motions (Andari et al., 2010; Hollander et al., 2003; Hong et al., 2014; Kim et al.,
249 2016; Langen et al., 2011b, 2011a; Lewis et al., 2007); that is, repetitive behaviour seems to
250 antagonize social behaviour. This antagonistic relationship between social and repetitive
251 behaviours has rarely been reported in other vertebrates. In cavefish, we observed a highly biased
252 one-way turning, based on the ratio of the numbers of left and right turns occurring per fish in
253 each 0.25-s interval, during the 5-min recording (Figure 4A, C and E). There was, however, no
254 detectable left-right preference in the direction of turning among individual cavefish (Figure 4C).
255 In contrast, surface fish showed symmetrical and balanced turning tendencies (Figure 4B and D).
256 As with cavefish, there was no significant left or right preference in the turning direction in
257 surface fish (Figure 4B). The levels of bias and direction preference were consistent for each
258 individual cavefish over at least 10 days, indicating that biased turning is a stable phenotype
259 (interclass correlation: kappa = 0.92, P = 0.0016, N = 6) (Shrout and Fleiss, 1979) (Figure 4—
260 figure supplement 1). Using this biased turning index, we analysed its relationship with the new
261 unfamiliar environment and nearby interactions.
262 In mammals, stereotypic repetitive motion is enhanced within novel unfamiliar
263 environments (Boulter et al., 2014; Buhr and Dugas, 2009). Cavefish showed high levels of

264 repetitive turning behaviour in both familiar and unfamiliar environments, where a shift in the
265 level was not detectable (Figure 3E, Supplementary File 1). Additionally, surface fish showed
266 less repetitive turning in both the familiar and unfamiliar environments (Figure 3E,
267 Supplementary File 1). We therefore concluded that biased turning is a stable phenotype under
268 these two tested environments.

269 We then tested whether repetitive turning was associated with reduced social-like
270 interaction in cavefish. We did not include surface fish in this correlation analysis because
271 surface fish showed almost no variation in repetitive turning (Figure 3E). By fitting a logarithmic
272 curve, based on a logarithmic conversion in the turning bias index, significant correlations
273 between turning bias and duration and between turning bias and nearby-interaction bout number
274 were detected in cavefish in the familiar environment ($R^2 = 0.198$, $P = 0.0038$; $R^2 = 0.204$, $P =$
275 0.0033, respectively; Figure 5A and B). However, in the unfamiliar environment, where the
276 nearby interactions were reduced in cavefish, no or less significant correlations between nearby
277 interactions and turning bias was detected ($R^2 = 0.069$, $P = 0.0659$ and $R^2 = 0.094$, $P = 0.0384$,
278 respectively; Figure 5C and D), possibly due to the significantly reduced variation in nearby
279 interactions.

280 In summary, a negative correlation between social-like nearby interactions and restricted
281 repetitive behaviour was revealed in cavefish under non-stressful conditions. This relationship is
282 shared between mammals and cavefish (Boulter et al., 2014; Buhr and Dugas, 2009; Kim et al.,
283 2016, and personal communication with Dr. Ryan Lee). Additionally, the reduction in nearby
284 interactions in an unfamiliar environment in cavefish was similar to that in mammals (Boulter et
285 al., 2014; Buhr and Dugas, 2009; Kim et al., 2016), suggesting the possibility of shared neural
286 processing between fish and mammals in these behavioural expressions.

287

288 Involvement of the dopaminergic system in the balance between levels of nearby interactions
289 and turning bias

290 In mammals, one of the brain regions involved in the expression of restricted repetitive
291 behaviour is the striatum (Kim et al., 2016; Langen et al., 2011b; Lewis et al., 2007). The
292 cortico-striatal system is thought to be deeply conserved from teleosts to mammals, and
293 dopaminergic inputs from the ventral tegmental area (VTA) and substantia nigra pars compacta
294 (SNpc) play an important role in behavioural choice in this system (Grillner and Robertson,
295 2016; Kim et al., 2016; Stephenson-Jones et al., 2011). Within the striatum, the balance between
296 the D1 direct and D2 indirect pathways is crucial, from lamprey to mammals, in balancing
297 behaviours (Grillner and Robertson, 2016; Kim et al., 2016; Stephenson-Jones et al., 2011). An
298 antipsychotic drug, aripiprazole, is one of two approved drugs for ASD treatment by the U.S.
299 Food and Drug Administration (FDA). Aripiprazole suppresses the phasic stimulation-dependent
300 activity of the indirect D2 pathway but preserves the basal tonic level of the D2 indirect pathway
301 due to its partial antagonistic action on the D2 receptor in mammals (de Bartolomeis et al.,
302 2015). Aripiprazole is prescribed to reduce irritability, perhaps because it maintains the basal
303 inhibitory activities of the D2 pathway and reduces repetitive behaviours (de Bartolomeis et al.,
304 2015). To address whether there is a parallel response to this drug between *A. mexicanus* and
305 humans, we treated surface fish and cavefish with aripiprazole through bath application and
306 tested whether the treatment affected social-like nearby interactions and repetitive turning in both
307 surface fish and cavefish.

308 Consistent with our previous findings (Yoshizawa et al., 2018), both surface fish and cavefish
309 had lower overall swimming distance travelled following aripiprazole treatment compared to the

310 control or pre-treatment levels ($X^2(1) = 17.4$, $P = 3.05\times10^{-5}$; Figure 6A, Supplementary File 1).
311 Following this treatment, cavefish showed reduced repetitive biased turning ($W = 642$, $P =$
312 0.0170; Figure 6B, Supplementary File 1) and increased social-like nearby interactions ($W =$
313 279, $P = 0.0375$; Fig 6C, Supplementary File 1). Surface fish did not show changes in either
314 repetitive biased turning or social-like nearby interactions ($P > 0.05$; Figure 6B, C and D;
315 Supplementary File 1). Aripiprazole treatment did not change the profile of velocity shifts during
316 the bout in either surface fish or cavefish: surface fish did not reduce the swimming speed during
317 bouts; in contrast, cavefish reduced swimming speed during bout compared with other periods
318 (surface fish PrePost × Treat × Speed: $X^2(3) = 0.4$, $P = 0.9431$; cavefish PrePost × Treat ×
319 Speed: $F_{3,140} = 1.5$, $P= 0.2073$; Figure 6E and F, Supplementary File 1).
320 To test whether the overall activity reduction itself is the factor that induced the duration and
321 number of interaction bouts, we performed correlation analyses between swimming speeds and
322 nearby-interaction durations. Swimming speed was not a significant predictor of nearby
323 interactions in either surface fish or cavefish pre- or post-aripiprazole treatment ($P > 0.05$; Figure
324 6—figure supplement 1). These results suggested that aripiprazole induced nearby interactions in
325 cavefish not only because of reductions in the swimming speed.
326

327 **Discussion**

328 In this study, we document that the sighted surface-dwelling form of *Astyanax mexicanus* is able
329 to follow and interact with conspecifics in the dark. We also reveal that so-called 'asocial'
330 cavefish retain a low but detectable level of ability to engage in social-like interactions. The
331 social-like interaction depended on the familiarity to the environment, and interestingly, surface
332 fish and cavefish showed opposite responses to the environments: in the familiar environment,
333 cavefish showed more social-like nearby interactions, while surface fish showed reduced social
334 interaction; in contrast, in the unfamiliar environment, surface fish tended to exhibit a longer
335 duration of nearby interaction, while cavefish exhibited a reduced duration of nearby interaction.
336 Cavefish also showed a significant negative correlation between the levels of repetitive turning
337 behaviour and social-like interactions in the familiar environment. This quantitative antagonistic
338 relationship between repetitive behaviour and social-like interactions has been reported in studies
339 involving humans and rodents (Boulter et al., 2014; Buhr and Dugas, 2009; Hong et al., 2014),
340 but there are few reports in teleosts. Treatment with the partial D2 receptor antagonist
341 aripiprazole enhanced social-like interactions and suppressed repetitive turning in cavefish,
342 which is consistent with aripiprazole treatment results in human patients (de Bartolomeis et al.,
343 2015; Ghanizadeh et al., 2014; Nasrallah, 2008).

344

345 In terms of measuring collective behaviours, the current definition of nearby interaction
346 is close to that of 'attraction' in zebrafish larvae under lighted conditions (Hinz and De Polavieja,
347 2017) (for a more general definition, see Lukeman et al., 2010), and we believe these two indices
348 indicate the same interactions. However, we could not apply Hinz's criteria to ours because they
349 used larval fish (~24 days post fertilization: 0.6 cm in body length; Parichy et al., 2009). Larval

350 fish swim in a highly viscous low Reynolds number-fluid environment (Vogel, 1983) where the
351 larval fish do not glide. Thus, the turning direction that Hinz et al. measured was sufficient to
352 measure collective behaviour. In contrast, we used young adult fish (1.5-2.0 cm), who swam in a
353 higher Reynolds number-fluid environment and glided while swimming. Therefore, this measure
354 of nearby duration that results from the manoeuvring efforts of the fish was more appropriate for
355 representing the level of collective behaviour than simply measuring the turning direction.
356
357 The majority of studies on shoaling and schooling behaviours of teleost fish have been
358 conducted under environmental conditions where visual cues predominate, potentially
359 exaggerating the importance of the visual system in these behaviours (Larsch and Baier, 2018).
360 Observations of the maintenance of shoaling behaviour in blinded fishes support the involvement
361 of lateral line mechanosensing; however, few studies have used intact fish to test the
362 involvement of the lateral line (Partridge and Pitcher, 1980; Pitcher, 1979; Pitcher et al., 1976).
363 Furthermore, many shoaling tests have been conducted in somewhat physically constrained
364 conditions (e.g., using a transparent glass divider between stimulus fish and test fish (Dreosti et
365 al., 2015) or using a small mesh cage that constrains the swimming area of the stimulus fish
366 (Gerlai, 2014)), where the true extent of mechanosensing in the control of shoaling behaviour
367 may be underplayed. In this study, we conducted the first systemic analysis of social-like nearby
368 interactions in intact fish under free-swimming conditions in the dark.
369 Using our method of measuring nearby interactions via idTracker-based tracking of each
370 individual, a 'nearby interaction' was defined by both a threshold maximum proximity distance
371 between two fish (≤ 5 cm) and a minimum threshold interaction duration (≥ 4 s). This method
372 was sensitive enough to detect changes in nearby interactions in different environments (e.g.,

373 familiar and unfamiliar; Figure 3) and following drug treatment (Figure 6; Figure 3—figure
374 supplement 2). This method is also applicable to measure a unit of collective behaviour among
375 larger groups (i.e., two fish attractions or nearby interactions among ≥5 individuals) in other
376 animal species.

377 Regarding non-visual collective behaviour in *A. mexicanus*, a quantitative trait locus
378 (QTL) for non-visual schooling has been reported where F_2 hybrid fish generated from a pair of a
379 surface fish and a Tinaja cavefish (a cave population that evolved independently from that of the
380 Pachón cave; Pachón cavefish were used in this study) were used (Kowalko et al., 2013). The
381 schooling measurement was based on how the F_2 individual responded to the school of 'model
382 fish' and based on NND. The major schooling QTL is associated with vision (Kowalko et al.,
383 2013). The QTL for non-visual schooling was detected by using only F_2, which showed negative
384 phototaxis (i.e., had visual capacity) but exhibited large differences from non-schooling to
385 schooling . The method presented here can improve the detection resolution in terms of nearby
386 interactions. Regardless, it was interesting that F_2 individuals carrying homozygous cave
387 genotypes at a marker underlying this QTL exhibited increased schooling behaviour, while F_2
388 individuals with homozygous surface or heterozygous genotypes schooled less (Kowalko et al.,
389 2013). This genetic study suggests two possibilities: (1) Tinaja cavefish evolved a 'schooling
390 allele', which is different from the 'nearby interaction alleles' that Pachón cavefish have, or (2)
391 the same allele regulates Tinaja's schooling behaviour and Pachón's nearby interaction. Note
392 that Tinaja's schooling allele may simply be an appetite-driving gene since aggression or
393 foraging against fish plastic models was not evaluated in the former study (Kowalko et al.,
394 2013), and Tinaja cavefish show insatiable appetites (Aspiras et al., 2015) (see below for

395 cannibalistic foraging). Based on this complexity, a crossing experiment between Tinaja and
396 Pachón cavefish is necessary to answer these possibilities.

397 Based on our results of pharmacological ablation of the lateral line, the nearby interaction
398 of surface fish in the dark is likely regulated by lateral line mechanosensors (Figure 2—figure
399 supplement 4). However, this result does not mean that the involvement of other sensory
400 systems, such as tactile and olfactory systems, can be excluded (Timmermann et al., 2004).
401 Further tests are needed to address which of these sensory systems plays the crucial role in
402 regulating nearby interactions in fish in the dark.

403 In the dark, surface fish changed their swimming direction based on the presence of other
404 individuals, as if they sensed and were attracted to others, similar to what has been observed in
405 zebrafish larvae under lighted conditions (Figure 2—figure supplement 2) (Hinz and De
406 Polavieja, 2017). However, surface fish failed to form a clear cluster, *i.e.*, a 'shoal', in the dark.
407 Instead, surface fish individually responded to one another. We believe that the failure to form a
408 shoaling cluster was based on the lack of visual information (see Videos 2 and 3 under light and
409 dark conditions, respectively), yet surface fish maintained their collective tendency in the dark
410 by using lateral line sensing.

411 The nearby interactions detected in this study did not appear to be related to foraging
412 activities or aggression (*i.e.*, two fish come close while expressing aggression or cannibalistic
413 foraging (Elipot et al., 2013)). We categorized the nearby activities into five classes of activity
414 and visualized them to show the frequent role changes of leaders and followers within single
415 bouts in the same fish pair (Figure 2–figure supplement 2C and E). This role change is rarely
416 observed in aggressive encounters (Elipot et al., 2013). In addition, cavefish slowed during the
417 nearby-interaction bout compared with other periods of time, which contradicts the speed shift

418 observed during aggression—fish thrust during aggression (Elipot et al., 2013). Finally, we
419 carefully assessed damage to the fins and scales, and although these tissues are good indicators
420 of aggressive encounters, noticeable damage was not detected. Consistent with this observation,
421 both surface fish and cavefish rarely showed startle responses after touching one another. We
422 therefore conclude that *A. mexicanus* rarely attacked one another in our assay system and that the
423 majority of detected nearby interactions can be characterized as shoaling-like activities.

424 The degree and type of nearby interactions in the dark that were recorded in this study
425 appear relevant within the context of each morph's natural habitat. Surface fish have a known
426 nocturnal predator, prawn fish (Wilson et al., 2004), and adult surface fish form a tighter
427 shoaling cluster at night (personal observation in the laboratory). These facts imply that shoaling
428 can be advantageous by simply lowering individual risk among cohorts, the so-called 'attack
429 dilution effect', and/or by increasing sensitivity in detecting potential predators by the collective
430 effect of more sensors of multiple individuals (Pitcher and Parrish, 1993). In cavefish, a higher
431 level of nearby interactions detected in the familiar laboratory setting was also observed in their
432 natural habitat, Cueva de El Pachón, Tamaulipas, Mexico (2019, personal observation). While
433 they did not form a recognizable shoal, cavefish responded to conspecifics and tended to follow
434 each other. This social-like tendency could merely be a residual of regressive evolution to a
435 troglobitic niche following their divergence from surface riverine ancestors (Langecker et al.,
436 1991; Yoshizawa et al., 2012). Alternatively, this weak social-like tendency could remain
437 advantageous for finding mates, locating food or evading potential dangers within their cave
438 environment.

439 The young adult surface fish used in this study had reached an appropriate developmental stage
440 to express the shoaling behaviour, and all of their behaviours were assessed only in the day.

441 Since the shoaling motivation was seen at night with very limited visual inputs (see above), it is
442 important to investigate shoaling capacity at night in future studies.
443 In the unfamiliar setting, the cavefish reduced the social-like interaction and kept high-level of
444 repetitive turning, suggesting that cavefish lost the strategy to use social-like interactions to
445 confront unfamiliar environmental inputs, which surface fish have.
446
447 Restricted repetitive behaviours are observed in mammals kept in restricted/isolated
448 environments and in humans with stereotypic movement disorders, including ASD (Lewis et al.,
449 2007; Rose et al., 2017). This motor disorder has been considered non-functional. However,
450 since these stereotypic behaviours are seen in many vertebrate species as well as in normally
451 developing human infants, there may be an advantage to repetitive behaviours. To understand the
452 behavioural function of repetitive motion, an emerging hypothesis—predictive processing—was
453 introduced in cognitive neuroscience (Palmer et al., 2017). In this framework, to develop an
454 internal model for the habitat (= environment), the central nervous system is continuously
455 attempting to minimize prediction errors, that is, differences between the environmental signals
456 sampled by an animal's sensory systems and that animal's internal model of the world within the
457 brain. The brain is assumed to have two strategies to minimize differences between sensory input
458 and the internal model when novel stimuli are encountered: (i) to use a better fitting model
459 among many existing internal models or (ii) to locomote back to a 'no-novel stimulus
460 environment' to sample the sensory inputs that had already been implemented in the current
461 internal model (Friston, 2010). Stereotypic repetitive circling seems to be a result of choosing the
462 latter strategy by sampling predictable sensory inputs (strong lateral line inputs on one side of the
463 body). This method can reduce the prediction errors between the sensory inputs and those

464 predictions from the internal model (*e.g.*, left turning provides the strong right lateral line signals
465 in cavefish). In contrast, surface fish responded to unfamiliar stimuli and did not increase
466 repetitive turning, perhaps by selecting a better fitting model among the available internal models
467 (*i.e.*, strategy (i)). Therefore, based on this predictive processing framework, surface fish and
468 cavefish apparently have different strategies. Both of these changes could minimize the errors
469 between the sensory inputs and the predicted inputs associated with the internal model. Given
470 that surface fish appear to acclimatize to novel environments much quicker than cavefish
471 measured by foraging latency (personal observation), this suggests that surface fish may store
472 many internal models that are proxies of the current environment. Having many internal models
473 is thought to better highlight new salient stimuli in a changing environment (i.e., a good fitting-
474 internal model yields better attention to the new object). The difference in the richness of internal
475 models between surface fish and cavefish is addressable by examining relationships between a
476 number of different environmental setups and how individuals can accurately navigate to reach
477 food without panicking/repetitive motion.
478
479 Previous studies have indicated that there is an antagonistic relationship between repetitive and
480 social behaviour (Kim et al., 2016; Lewis et al., 2007). For example, social impairment and
481 repetitive behaviour are thought to be linked together as revealed by results following oxytocin
482 infusion (reviewed in (Kim et al., 2016)). In contrast, in a study of ketogenic diet treatment in
483 individuals with autism, social behaviour in some treated patients had recovered to normative
484 levels, while repetitive behaviour was not significantly attenuated (Lee et al., 2018). This result
485 suggested that repetitive behaviour can be independent of social impairment. The mechanisms
486 that controls switching between social and repetitive behaviours is still largely unknown. Many

487 studies of repetitive behaviour and social behaviour have focused on the cortico-striatal system,
488 where many patients who show repetitive behaviour (including those with Gilles de la Tourette
489 syndrome, obsessive–compulsive disorder, ASDs, Parkinson's disease, and Huntington's disease)
490 have abnormal functional and/or histological features diagnosed by PET and fMRI (Langen et
491 al., 2011a). Importantly, this striatal system, particularly its dopaminergic system, has also been
492 suggested to drive social behaviour, where the dopamine signal from the VTA stimulates D1-
493 dopamine receptor-positive striatal neurons in the nucleus accumbens, driving social behaviour
494 in mice (Gunaydin et al., 2014; Kim et al., 2016). Among vertebrates, the striatum has been
495 proposed as the conserved bridging centre. The striatum integrates (1) higher levels of sensory
496 inputs from the cerebral cortex/dorsal pallium and (2) information-evaluating dopaminergic input
497 from the substantia nigra par compacta (SNc). The dopaminergic striatal pathway is largely
498 conserved among vertebrate species. This includes the direct and indirect pathways, each of
499 which is associated with a specific type of dopamine receptor—D1 and D2 receptors,
500 respectively. The major function of this striatal dopaminergic system is thought to be to select
501 behavioural modules (*e.g.*, mating, foraging, and aggression modules) based on given sensory
502 inputs and internal states (Grillner, 2018; Grillner and Robertson, 2016). For example, a fish may
503 ignore or follow mechanical signals from cohorts based on the fish's internal state.
504 In addition to the striatal behaviour switching centre, many other brain regions are known to
505 induce social/social-like behaviours. For example, from teleosts to mammals, the best
506 neurochemically conserved social decision-making network has been reported to be the preoptic
507 area (POA based on an analysis of 10 gene products across 12 brain decision-making processing
508 regions in 88 species; dopaminergic neurons also exist in this region) (O'Connell and Hofmann,
509 2012, 2011).

510 Accordingly, bath treatment with a partial D2-dopamine receptor antagonist, aripiprazole,
511 showed a parallel response between cavefish and humans, suggesting a potential shared pathway
512 that controls social-like and repetitive behaviours in teleosts and mammals and possibly involves
513 the striatum, POA, and/or other dopaminergic processing nuclei (Grillner, 2018; Kim et al.,
514 2016; O'Connell and Hofmann, 2011). Future studies will address whether the antagonistic
515 relationship between social-like and repetitive behaviours is based on the switch of behaviour
516 modules in the striatal system or whether repetitive motions simply fragment social-like
517 interactions, although the individual may continue to have the motivation to congregate.
518 It will be exciting to examine the evolutionary and neurophysiological changes in the
519 dopaminergic system between cavefish and surface fish and how these changes are associated
520 with the integration of an internal model, which the predictive-processing theory proposes, in the
521 future.
522
523

524 **Materials and Methods**

525 Fish maintenance and rearing in the laboratory

526 The *Astyanax mexicanus* surface fish used in this study were laboratory-raised descendants
527 of original collections made in Balmorhea Springs State Park, Texas, by Dr. William R. Jeffery.
528 The cavefish were laboratory-raised descendants originally collected from Cueva de El Pachón in
529 Tamaulipas, Mexico by either Drs. William R. Jeffery or Richard Borowsky.

530 Fish (surface fish and Pachón cave populations) were housed at the University of Hawai‘i at
531 the Mānoa aquatic facility with temperatures set at 21°C ± 0.5°C for rearing, 22°C ± 0.5°C for
532 behavioural experiments, and 25°C ± 0.5°C for breeding (Elipot et al., 2014; Yoshizawa et al.,
533 2015). Lights were maintained on 12:12 light:dark cycles (Elipot et al., 2014; Yoshizawa et al.,
534 2015). For rearing and behavioural experiments, light intensity was maintained between 30-100
535 lux. Fish were raised to 7-12-month-old young adults and maintained in plastic containers
536 (Ziplock® containers, S. C. Johnson & Son, Inc., Racine, WI, USA) with ~20 cohorts. Young
537 adult fish were fed live brine shrimp nauplii to satiation two times daily starting 3 hours after the
538 lights came on (Zeitgeber time 3 or ZT3) and ZT9 (Premium Grade Brine Shrimp Eggs, Brine
539 Shrimp Direct, Ogden, UT, USA). All fish in the behavioural experiments were between 3-4 cm
540 in standard length and between 7-12 months old. Regarding the selection of experimental fish, as
541 often as possible, all the fish groups in our study comprised age-matched siblings. We then equally
542 mixed age-matched individuals from different parents within the morph (cavefish or surface fish)
543 when we had a shortage of siblings. We did not exclude any outliers from our dataset except those
544 showing atypical pre-treatment behaviours (see the Statistical analysis section below). All fish care
545 and experimental protocols were approved by the IACUC (17-2560) at the University of Hawai‘i

546 at Mānoa. All populations of *A. mexicanus* used in this study are readily available from us upon
547 request.
548
549 Recording fish group behaviour
550 Prior to experimentation, four fish comprising group-raised siblings were housed in a "home"
551 container (15.6 × 15.6 × 5.7 cm: Ziplock® containers, S. C. Johnson & Son, Inc.) filled with
552 conditioned water (pH 6.7-7.3; conductivity 600-800 µS) for four or more days. Fish were fed
553 twice a day with live brine shrimp nauplii until the morning of the recording. For the unfamiliar
554 environment experiment, all four fish were gently transferred to a 37.85 L tank (50.8 × 25.4 ×
555 30.5 cm) with a water depth of 2 cm on the stage of a custom-made infrared (IR) back-light
556 system within a custom-built black box (75 × 50 × 155 cm, assembled with polyvinyl chloride
557 (PVC) pipe frame and covered by shading film). The IR back-light system was composed of
558 bounce lighting of IR LED strips (SMD3528 850-nm strip: LightingWill, Guang Dong, China)
559 (Figure 1A). Videos were recorded using a USB webcam (LifeCam Studio 1080p HD Webcam,
560 Microsoft, Redmond, WA, USA) fitted with a c-mount zoom lens (macro 1.8/12.5-75 mm C-
561 mount zoom lens, Toyo Lens, Tokyo, Japan) installed on the top of the custom-built black box.
562 An IR high-pass filter (Optical cast plastic IR long-pass filter, Edmund Optics Worldwide,
563 Barrington, NJ, USA) was placed between the camera and the lens to block visible light. The
564 video was captured at 20 frames per second using VirtualDub software (version 1.10.4,
565 http://www.virtualdub.org/) or VirtualDub2 (build 44282,
566 https://sourceforge.net/projects/vdfiltermod/) with a vfw codec
567 (https://sourceforge.net/projects/x264vfw/). After 6 min of recording, the fish were returned to
568 the housing container. For the familiar environment experiment, fish were transferred to 37.85 L

569 tank (50.8 × 25.4 × 30.5 cm) with a water depth of 2 cm and kept for four days to let them
570 acclimate. On the fourth day, prior to the recording, we monitored the water qualities of each
571 tank (pH, conductivity, and ammonia, nitrite, and nitrate levels) and then performed the
572 recording in tanks with healthy water conditions (i.e., pH = 6.7-7.3, conductivity = 680-800 μS,
573 almost 0 in ammonia, nitrite and nitrate levels). All tanks met these criteria. The movements of
574 the acclimated fish were recorded using the same acclimation tank and water. After all recording
575 sessions, the study fish were visually checked for damage to the fins and for lost scales as an
576 indicator of overt aggression.
577
578 Drug treatment
579 The bath treatment of aripiprazole (Selleck, Houston, TX) was performed as described in
580 Yoshizawa et al. (Yoshizawa et al., 2018). Briefly, the aripiprazole working solution was
581 prepared by mixing 1.0 mM aripiprazole stock solution into fish-conditioned water to make a
582 1,000 × dilution (final concentration: 1.0 μM aripiprazole and 0.01% DMSO in the conditioned
583 water). For the stock solution, aripiprazole (Selleck, Houston, TX) was dissolved in 100%
584 dimethyl sulfoxide (DMSO, Millipore Sigma). For the control, 0.01% DMSO in conditioned
585 water was used. The four fish in each home container were treated with either the aripiprazole
586 working solution or the 0.01% DMSO control solution overnight (~16 hours). The next morning,
587 the fish group behaviours in the 37.85 L tank were recorded as described in the "Recording fish
588 group behaviour" section.
589
590 Tracking

591 The first minute of each original video was discarded since this time interval contains the
592 moment that four fish were released from their home container, which agitated the water surface,
593 disrupting observation. Before tracking each fish's position by idTracker software (Pérez-
594 Escudero et al., 2014), the background visual artefacts were subtracted by a custom-made ImageJ
595 macro script. Briefly, with videos recorded with a white background, each frame image was
596 adjusted by the "Add" operation of the 'Image Calculator' function with an inverted median z-
597 stacked image of 2,000 frames calculated by 'Z Project...' and 'Invert' functions of ImageJ
598 (Schneider et al., 2012). Then, the frame images' contrasts were adjusted based on each video.
599 Each processed video was saved in AVI format by using jpeg compression in ImageJ. Using
600 these background-subtracted videos, the X-Y coordinates of each fish were extracted by tracking
601 each fish's ID under the ID-detection algorithm of idTracker (idTracker-beta running under
602 MATLAB release 2019a or above (https://github.com/idTracker/idTracker/tree/Beta) (Pérez-
603 Escudero et al., 2014) (The MathWorks Inc., Natick, MA, USA). The parameters of idTracker
604 were usually set as follows: number of individuals, 4; intensity threshold, 0.75-0.89; minimum
605 size, 50; "select region by polygon" function enabled; and "Remove background" option
606 checked. We aimed to achieve a successful tracking frame ratio above 97% by adjusting these
607 parameters. Even with a high ratio of successful tracking frames (*e.g.*, 99%), the outputs of
608 idTracker can contain ID errors by switching the IDs between different fish. These errors were
609 manually surveyed frame-by-frame by using idPlayer, an accompaniment to idTracker software
610 (Pérez-Escudero et al., 2014). The corrected IDs were re-assigned by a custom Python script
611 (https://zenodo.org/record/5122894#.YPnDBR1ujsF). If a fish had periods without an ID during
612 the analysed videos, the estimated X-Y coordinates were calculated for those durations by
613 averaging velocity and swimming direction between the X-Y coordinates before and after the

missing ID period. Tracking results were used for the repetitive turning and nearby-interaction analyses (see below).

Biased repetitive turning analyses

Changes in the angles in swimming directions in every 5 frame windows (i.e., every 0.25 s) were calculated as radians. When the X-Y coordinates of the three time points (t_0, t_1, and t_2) were (x_0, y_0), (x_1, y_1) and (x_2, y_2), the swimming angle θ between two vectors ($x_1 - x_0$, $y_1 - y_0$) and ($x_2 - x_1$, $y_2 - y_1$) was calculated as the cross product of two vectors:

$$\theta = arctan \frac{(x_1-x_2)(y_0-y_1)-(y_1-y_2)(x_0-x_1)}{(x_1-x_2)(x_0-x_1)+(y_1-y_2)(y_0-y_1)}.$$

The numbers of frames that had negative radian values (N_1), representing clockwise turns, and positive radian values (N_2), representing anticlockwise turns, were totalled. The repetitive turning index was then calculated as $\log_2 N_1/N_2$. As fish did not show any preference in the direction of turning (Figure 4B and C, and Figure 4—figure supplement 1), the repetitive turning index was expressed as the absolute value of $\log_2 N_1/N_2$.

Recording of single fish repetitive behaviour

Repetitive behaviour assays were carried out with single fish; each individual fish was, in turn, transferred from the home container to a 25.5 x 38.0 cm Pyrex glass baking dish, filled to a water depth of ~4 cm, by using a fine brine shrimp net. Two of these dish arenas were lit by a custom-made IR light box from underneath (a 58.4 × 41.2 × 15.2 cm opaque storage box equipped with IR LED strip SMD3528 850-nm strip: LightingWill). Videos for this behavioural assay were recorded with the same camera setup as described in the “Recording fish group behaviour” section.

637 A repeated behavioural assay using the same fish was recorded 10 days after the first. To identify
638 individuals, each fish was labelled with a physically implanted dye (Visible Implant Elastomer
639 (VIE) tags, Northwest Marine Technology, Inc. Anacortes, WA, USA) while anaesthetized in a
640 bath treatment of ice-cold 0.2 mg/mL MS-222 (Millipore Sigma, St. Louis, MO), directly after
641 the first recording. After 10 days, the fish behaviour was recorded using the same procedure.
642
643 Social-like nearby-interaction analysis
644 The IIDs and NNDs were calculated according to Partridge et al. (Partridge et al., 1980). For the
645 IID measurement, the average of the distances between the four fish being assayed (6 distances)
646 was calculated per video frame. Then, the mean and standard error of means (s.e.m.) were
647 calculated by using one 4-fish group as N = 1 (for example, N = 18 in each of the surface fish
648 and cavefish experimental groups in Figure 2B). For the NND measurement, the average of the 4
649 nearest distances between a focal fish and the nearest individual per video frame was determined,
650 then the mean and s.e.m. were calculated as with the IIDs (Figure 2A).
651 A 'nearby-interaction bout' was defined by a minimum interaction duration threshold of four
652 seconds and a maximum physical distance threshold of 5-cm distance between the two fish.
653 Notably, the definition of nearby interaction is close to that of 'attraction' by Hinz et al., where
654 attraction was expressed as the probability that the focal turns to the side where the other fish is
655 located (Hinz and De Polavieja, 2017). The current nearby interaction measures the preference to
656 stay or follow one another without consideration of the turning direction. We use the term
657 'nearby interaction' in this study to avoid confusion (see Results section).
658 Nearby interactions were extracted from each fish's X-Y coordinates by a custom-made
659 MATLAB script. The bout duration was adjusted by subtracting the PbDur (see the following,

660 Supplementary File 2, and Figure 2—figure supplement 1C). PbDur was defined as the average
661 duration of a fish passing by another fish in a situation where these fish do not engage in a
662 nearby interaction. The purpose of subtracting the PbDur from the bout durations was to remove
663 the period from the nearby-interaction events that resulted simply from physical proximity rather
664 than the actual social-like interaction. PbDur was calculated as PbDur = 5 cm /V, where V was
665 the average speed of four fish in the same group during the 5-min period (Supplementary File 2;
666 Figure 2—figure supplement 1C). If V is low, PbDur becomes longer; therefore, the removal of
667 the PbDur excludes 'by-chance' events where two fish may remain within 5 cm of one another
668 while not expressing attraction towards one another. Subtraction of PbDur from each detected
669 bout was performed with all presented results including data across surface fish and cavefish,
670 environments, and drug treatments. The swimming velocities 'during the bout,' '4 s before bout
671 commencement,' and '4 s directly following the bout' were also extracted and calculated using a
672 custom-made MATLAB script.
673 A random sampling test was performed by random selection of one individual from each group
674 (i.e., one of four fish) and forming a simulated 4-fish group, where none of the individuals
675 physically swam in the same arena. We then calculated the IIDs (Figure 2D), the duration of
676 each IID event (Figure 2E), and the total nearby-interaction duration (Figure 2G) among these
677 simulated 4-fish groups by using their 5-min X-Y coordinates. The simulated 4-fish group was
678 randomly and exclusively formed 1,280 times for the tests in Figure 2D and E and 18 times for
679 Figure 2G by using each surface fish and cavefish dataset.
680
681 <u>Statistical analysis</u>

682 Regarding a power analysis, we designed our experiments based on 3-way repeated measures
683 ANOVA whose effect size was moderate (f = 0.25), with an alpha-error probability = 0.05 and
684 power = 0.80, and the number of groups was 8 (surface fish vs. cavefish × control vs. treated ×
685 pre- vs. post-treatment). G*Power software (Erdfelder et al., 2009; Faul et al., 2007) estimated
686 that the sample size needed for this experiment was N=9 per group. We thus designed to have N
687 ≥ 12 for all experiments in this study.
688 For statistical comparisons of our data, we performed tests including Student's *t*-tests and
689 Wilcoxon's signed-rank tests and two-way or three-way generalized linear model analyses to
690 compare surface vs. cavefish, treated vs. non-treated, and pre- vs. post-treatments. We calculated
691 Akaike's information criterion (AIC) for each linear and generalized linear model and chose the
692 model with the lowest AIC. The post hoc Holm correction was used to understand which
693 contrasts were significant (Holm, 1979).
694 Regarding replicates of experiments, we used different individuals for the replicates, i.e., 2 or 3
695 biological replicates/trials, by using different individuals in each trial. There was no repeated
696 usage of individual fish with the exception of examining familiar and unfamiliar experiments
697 (Figure 3). Under these conditions, we confirmed that the averages of each day's data were
698 statistically indistinguishable from each other. We then merged the data acquired on different
699 days and presented the data as a single set of results (*i.e.*, one biological replicate).
700 The above calculations were conducted using R version 4.0.4 software (packages of car, lme4,
701 and lmerTest) (Bates et al., 2015; Fox and Weisberg, n.d.; Kuznetsova et al., 2017), and all
702 statistical scores are available in Supplementary File 1, figure legends or the body text.
703

Data availability

The video datasets generated and/or analysed during the current study are available at the university's shared server and will be deposited to Zenodo. All program scripts used in this study and those demo codes have been uploaded at Zenodo and are available at https://zenodo.org/record/5122894#.YPnDBR1ujsF.

The authors declare no competing interest.

Acknowledgements

We thank C. Balaan for constructive comments regarding insights on social-like interactions in cavefish. We also thank A. Hudson for the English language edit and providing significant improvements in the logical flow of the final draft. We are grateful to V. Crystal, J. Choi, L. Lu, J. Nguyen, VFL. Fernandes, K. Lactaoen, M. Worsham, H. Hernandez, N. Doeden, J. Kato, A. Tran, M. Ito, R. Balmilero-Unciano, E. Doy, A. Martinez, and D. Mones for fish care assistance.

References

Andari E, Duhamel JR, Zalla T, Herbrecht E, Leboyer M, Sirigu A. 2010. Promoting social behavior with oxytocin in high-functioning autism spectrum disorders. *Proc Natl Acad Sci U S A* **107**:4389–4394. doi:10.1073/pnas.0910249107

Aspiras AC, Rohner N, Martineau B, Borowsky RL, Tabin CJ. 2015. Melanocortin 4 receptor mutations contribute to the adaptation of cavefish to nutrient-poor conditions. *Proc Natl Acad Sci U S A* **112**:9668–9673. doi:10.1073/pnas.1510802112

Bates D, Mächler M, Bolker BM, Walker SC. 2015. Fitting linear mixed-effects models using lme4. *J Stat Softw*. doi:10.18637/jss.v067.i01

Bilandžija H, Abraham L, Ma L, Renner KJ, Jeffery WR. 2018. Behavioural changes controlled by catecholaminergic systems explain recurrent loss of pigmentation in cavefish. *Proc R Soc B Biol Sci* **285**:20180243. doi:10.1098/rspb.2018.0243

Bilandžija H, Ma L, Parkhurst A, Jeffery WR. 2013. A potential benefit of albinism in Astyanax cavefish: Downregulation of the oca2 gene increases tyrosine and catecholamine levels as an alternative to melanin synthesis. *PLoS One* **8**:e80823. doi:10.1371/journal.pone.0080823

Bleckmann H. 1986. Role of the Lateral Line in Fish Behaviour In: Pitcher TJ, editor. The Behaviour of Teleost Fishes. London: Chapman & Hall. pp. 177–202. doi:10.1007/978-1-4684-8261-4_7

Boulter C, Freeston M, South M, Rodgers J. 2014. Intolerance of uncertainty as a framework for understanding anxiety in children and adolescents with autism spectrum disorders. *J Autism Dev Disord*. doi:10.1007/s10803-013-2001-x

Buhr K, Dugas MJ. 2009. The role of fear of anxiety and intolerance of uncertainty in worry: An experimental manipulation. *Behav Res Ther*. doi:10.1016/j.brat.2008.12.004

742 Coleman DM, Adams JB, Anderson AL, Frye RE. 2019. Rating of the effectiveness of 26
743 psychiatric and seizure medications for autism spectrum disorder: Results of a national
744 survey. *J Child Adolesc Psychopharmacol* **29**:107–123. doi:10.1089/cap.2018.0121
745 de Bartolomeis A, Tomasetti C, Iasevoli F. 2015. Update on the Mechanism of Action of
746 Aripiprazole: Translational Insights into Antipsychotic Strategies beyond Dopamine
747 Receptor Antagonism. *CNS Drugs* **29**:773–799. doi:10.1007/s40263-015-0278-3
748 Dreosti E, Lopes G, Kampff AR, Wilson SW. 2015. Development of social behavior in young
749 zebrafish. *Front Neural Circuits*. doi:10.3389/fncir.2015.00039
750 Duboué ER, Borowsky RL, Keene AC. 2012. β-adrenergic signaling regulates evolutionarily
751 derived sleep loss in the Mexican cavefish. *Brain Behav Evol* **80**:233–43.
752 doi:10.1159/000341403
753 Duboué ER, Keene AC, Borowsky RL. 2011. Evolutionary convergence on sleep loss in
754 cavefish populations. *Curr Biol* **21**:671–676. doi:10.1016/j.cub.2011.03.020
755 Elipot Y, Hinaux H, Callebert J, Rétaux S. 2013. Evolutionary shift from fighting to foraging in
756 blind cavefish through changes in the serotonin network. *Curr Biol* **23**:1–10.
757 Fox J, Weisberg S. n.d. An R companion to applied regression.
758 Friston K. 2010. The free-energy principle: A unified brain theory? *Nat Rev Neurosci*.
759 doi:10.1038/nrn2787
760 Fumey J, Hinaux H, Noirot C, Thermes C, Rétaux S, Casane D. 2018. Evidence for late
761 Pleistocene origin of Astyanax mexicanus cavefish. *BMC Evol Biol* **18**:43.
762 doi:10.1186/s12862-018-1156-7
763 Gerlai R. 2014. Social behavior of zebrafish: From synthetic images to biological mechanisms of
764 shoaling. *J Neurosci Methods* **234**:59–65. doi:10.1016/j.jneumeth.2014.04.028

765 Ghanizadeh A, Sahraeizadeh A, Berk M. 2014. A head-to-head comparison of aripiprazole and
766 risperidone for safety and treating autistic disorders, a randomized double blind clinical
767 trial. *Child Psychiatry Hum Dev* **45**:185–192. doi:10.1007/s10578-013-0390-x
768 Grillner S. 2018. The Enigmatic "Indirect Pathway" of the Basal Ganglia: A New Role. *Neuron*
769 **99**:1105–1107. doi:10.1016/j.neuron.2018.08.040
770 Grillner S, Robertson B. 2016. The Basal Ganglia Over 500 Million Years. *Curr Biol* **26**:R1088–
771 R1100. doi:10.1016/j.cub.2016.06.041
772 Gunaydin LA, Grosenick L, Finkelstein JC, Kauvar I V., Fenno LE, Adhikari A, Lammel S,
773 Mirzabekov JJ, Airan RD, Zalocusky KA, Tye KM, Anikeeva P, Malenka RC, Deisseroth
774 K. 2014. Natural neural projection dynamics underlying social behavior. *Cell* **157**:1535–
775 1551. doi:10.1016/j.cell.2014.05.017
776 Herman A, Brandvain Y, Weagley J, Jeffery WR, Keene AC, Kono TJY, Bilandžija H,
777 Borowsky R, Espinasa L, O'Quin K, Ornelas-García CP, Yoshizawa M, Carlson B,
778 Maldonado E, Gross JB, Cartwright RA, Rohner N, Warren WC, McGaugh SE. 2018. The
779 role of gene flow in rapid and repeated evolution of cave-related traits in Mexican tetra,
780 *Astyanax mexicanus*. *Mol Ecol* **27**:4397–4416. doi:10.1111/mec.14877
781 Hinz RC, De Polavieja GG. 2017. Ontogeny of collective behavior reveals a simple attraction
782 rule. *Proc Natl Acad Sci U S A* **114**:2295–2300. doi:10.1073/pnas.1616926114
783 Hollander E, Novotny S, Hanratty M, Yaffe R, DeCaria CM, Aronowitz BR, Mosovich S. 2003.
784 Oxytocin infusion reduces repetitive behaviors in adults with autistic and asperger's
785 disorders. *Neuropsychopharmacology* **28**:193–198. doi:10.1038/sj.npp.1300021
786 Holm S. 1979. A simple sequentially rejective multiple test procedure. *Scand J Stat*.
787 Hong W, Kim DW, Anderson DJ. 2014. Antagonistic control of social versus repetitive self-

788 grooming behaviors by separable amygdala neuronal subsets. *Cell* **158**:1348–1361.
789 doi:10.1016/j.cell.2014.07.049
790 Jaggard JB, Stahl BA, Lloyd E, Duboue ER, Keene AC, Prober DA, Duboue ER, Keene AC.
791 2017. Hypocretin underlies the evolution of sleep loss in the Mexican cavefish. *Elife* **7**.
792 doi:10.7554/eLife.32637
793 Jørgensen JM. 1989. Evolution of Octavolateralis Sensory Cells BT - The Mechanosensory
794 Lateral Line In: Coombs S, Görner P, Münz H, editors. New York, NY: Springer New
795 York. pp. 115–145.
796 Kaplan G, McCracken JT. 2012. Psychopharmacology of Autism Spectrum Disorders. *Pediatr*
797 *Clin North Am* **59**:175–187. doi:10.1016/j.pcl.2011.10.005
798 Kazdoba TM, Leach PT, Yang M, Silverman JL, Solomon M, Crawley JN. 2016. Translational
799 mouse models of autism: Advancing toward pharmacological therapeutics. *Curr Top Behav*
800 *Neurosci* **28**:1–52. doi:10.1007/7854_2015_5003
801 Keene AC, Yoshizawa M, McGaugh SE. 2016. Biology and Evolution of the Mexican Cavefish,
802 Biology and Evolution of the Mexican Cavefish. Amsterdam: Elsevier Inc.
803 doi:10.1016/C2014-0-01426-8
804 Kim H, Lim CS, Kaang BK. 2016. Neuronal mechanisms and circuits underlying repetitive
805 behaviors in mouse models of autism spectrum disorder. *Behav Brain Funct*.
806 doi:10.1186/s12993-016-0087-y
807 Kowalko JE, Rohner N, Rompani SB, Peterson BK, Linden TA, Yoshizawa M, Kay EH, Weber
808 J, Hoekstra HE, Jeffery WR, Borowsky R, Tabin CJ. 2013. Loss of schooling behavior in
809 cavefish through sight-dependent and sight-independent mechanisms. *Curr Biol* **23**:1874–
810 83. doi:10.1016/j.cub.2013.07.056

811 Kuznetsova A, Brockhoff PB, Christensen RHB. 2017. lmerTest Package: Tests in Linear Mixed
812 Effects Models . *J Stat Softw*. doi:10.18637/jss.v082.i13
813 Langecker TG, Wilkens H, Junge P. 1991. Introgressive hybridization in the Pachón Cave
814 population of *Astyanax fasciatus* (Teleostei Characidae). *Ichthyol Explor Freshw* **2**:209–
815 212.
816 Langen M, Durston S, Kas MJH, van Engeland H, Staal WG. 2011a. The neurobiology of
817 repetitive behavior: ...and men. *Neurosci Biobehav Rev* **35**:356–365.
818 doi:10.1016/j.neubiorev.2010.02.005
819 Langen M, Kas MJH, Staal WG, van Engeland H, Durston S. 2011b. The neurobiology of
820 repetitive behavior: Of mice... *Neurosci Biobehav Rev* **35**:345–355.
821 doi:10.1016/j.neubiorev.2010.02.004
822 Larsch J, Baier H. 2018. Biological Motion as an Innate Perceptual Mechanism Driving Social
823 Affiliation. *Curr Biol* **28**:3523-3532.e4. doi:10.1016/j.cub.2018.09.014
824 Lee RWY, Corley MJ, Pang A, Arakaki G, Abbott L, Nishimoto M, Miyamoto R, Lee E,
825 Yamamoto S, Maunakea AK, Lum-Jones A, Wong M. 2018. A modified ketogenic gluten-
826 free diet with MCT improves behavior in children with autism spectrum disorder. *Physiol*
827 *Behav* **188**:205–211. doi:10.1016/j.physbeh.2018.02.006
828 Lewis MH, Tanimura Y, Lee LW, Bodfish JW. 2007. Animal models of restricted repetitive
829 behavior in autism. *Behav Brain Res* **176**:66–74. doi:10.1016/j.bbr.2006.08.023
830 Lukeman R, Li YX, Edelstein-Keshet L. 2010. Inferring individual rules from collective
831 behavior. *Proc Natl Acad Sci U S A* **107**:12576–12580. doi:10.1073/pnas.1001763107
832 Ma L, Parkhurst A, Jeffery WR. 2014. The role of a lens survival pathway including sox2 and
833 αA-crystallin in the evolution of cavefish eye degeneration. *Evodevo* **5**:28.

834 doi:10.1186/2041-9139-5-28

835 McGaugh SE, Gross JB, Aken B, Blin M, Borowsky R, Chalopin D, Hinaux H, Jeffery WR,
836 Keene A, Ma L, Minx P, Murphy D, O'Quin KE, Rétaux S, Rohner N, Searle SMJ, Stahl
837 BA, Tabin C, Volff JN, Yoshizawa M, Warren WC. 2014. The cavefish genome reveals
838 candidate genes for eye loss. *Nat Commun* **5**:5307. doi:10.1038/ncomms6307

839 Miller N, Greene K, Dydinski A, Gerlai R. 2013. Effects of nicotine and alcohol on zebrafish
840 (Danio rerio) shoaling, Behavioural Brain Research. doi:10.1016/j.bbr.2012.11.033

841 Montgomery J, Bleckmann H, Coombs S. 2013. Sensory ecology and neuroethology of the
842 lateral line In: Coombs S, Bleckmann H, Fay RR, Popper AN, editors. The Lateral Line
843 System. Springer Handbook of Auditory Research 48. New York: Springer. pp. 121–150.

844 Nasrallah HA. 2008. Atypical antipsychotic-induced metabolic side effects: Insights from
845 receptor-binding profiles. *Mol Psychiatry*. doi:10.1038/sj.mp.4002066

846 O'Connell LA, Hofmann HA. 2012. Evolution of a Vertebrate Social Decision-Making Network.
847 *Science (80-)* **336**:1154–1157. doi:10.1126/science.1218889

848 O'Connell LA, Hofmann HA. 2011. The Vertebrate mesolimbic reward system and social
849 behavior network: A comparative synthesis. *J Comp Neurol* **519**:3599–3639.
850 doi:10.1002/cne.22735

851 Palmer CJ, Lawson RP, Hohwy J. 2017. Bayesian approaches to autism: Towards volatility,
852 action, and behavior. *Psychol Bull* **143**:521–542. doi:10.1037/bul0000097

853 Parichy DM, Elizondo MR, Mills MG, Gordon TN, Engeszer RE. 2009. Normal table of
854 postembryonic zebrafish development: Staging by externally visible anatomy of the living
855 fish. *Dev Dyn* **238**:2975–3015. doi:10.1002/dvdy.22113

856 Partridge BL, Pitcher T, Cullen JM, Wilson J. 1980. The three-dimensional structure of fish

857 schools. *Behav Ecol Sociobiol* **6**:277–288. doi:10.1007/BF00292770

858 Partridge BL, Pitcher TJ. 1980. The sensory basis of fish schools: Relative roles of lateral line
859 and vision. *J Comp Physiol A* **135**:315–325. doi:10.1007/BF00657647

860 Patch A, Paz A, Holt K, Duboue E, Kowalko J, Keene A, Fily Y. 2020. Analysis of social
861 swimming dynamics in the Mexican cavefish. *bioRxiv* 2020.01.31.929323.
862 doi:10.1101/2020.01.31.929323

863 Patton P, Windsor S, Coombs S. 2010. Active wall following by Mexican blind cavefish
864 (*Astyanax mexicanus*). *J Comp Physiol A Neuroethol Sens Neural Behav Physiol* **196**:853–
865 867. doi:10.1007/s00359-010-0567-8

866 Pérez-Escudero A, Vicente-Page J, Hinz RC, Arganda S, De Polavieja GG. 2014. IdTracker:
867 Tracking individuals in a group by automatic identification of unmarked animals. *Nat*
868 *Methods* **11**:743–748. doi:10.1038/nmeth.2994

869 Pierre C, Pradère N, Froc C, Ornelas-García P, Callebert J, Rétaux S. 2020. A mutation in
870 monoamine oxidase (MAO) affects the evolution of stress behavior in the blind cavefish
871 Astyanax mexicanus. *bioRxiv* 2020.04.09.033266. doi:10.1101/2020.04.09.033266

872 Pitcher T. 1979. Sensory information and the organization of behaviour in a shoaling cyprinid
873 fish. *Anim Behav* **27**:126–149. doi:10.1016/0003-3472(79)90133-7

874 Pitcher TJ. 1973. The three-dimensional structure of schools in the minnow, *Phoxinus phoxinus*
875 *(L.)*. *Anim Behav* **21**:673–686. doi:10.1016/S0003-3472(73)80091-0

876 Pitcher TJ, Parrish JK. 1993. Functions of Shoaling Behaviour in Teleosts In: Pitcher TJ, editor.
877 Behaviour of Teleost Fishes. London: Chapman & Hall. pp. 363–440. doi:10.1007/978-1-
878 4684-8261-4_12

879 Pitcher TJ, Partridge BL, Wardle CS. 1976. A blind fish can school. *Science (80-)* **194**:963–965.

880 doi:10.1126/science.982056

881 Riddle MR, Aspiras AC, Gaudenz K, Peuß R, Sung JY, Martineau B, Peavey M, Box AC, Tabin
882 JA, McGaugh S, Borowsky R, Tabin CJ, Rohner N. 2018. Insulin resistance in cavefish as
883 an adaptation to a nutrient-limited environment. *Nature* **555**:647–651.
884 doi:10.1038/nature26136

885 Rohner N, Jarosz DFDF, Kowalko JEJE, Yoshizawa M, Jeffery WRWR, Borowsky RLRL,
886 Lindquist S, Tabin CJCJ. 2013. Cryptic variation in morphological evolution: HSP90 as a
887 capacitor for loss of eyes in cavefish. *Science (80-)* **342**:1372–1375.
888 doi:10.1126/science.1240276

889 Rose PE, Nash SM, Riley LM. 2017. To pace or not to pace? A review of what abnormal
890 repetitive behavior tells us about zoo animal management. *J Vet Behav Clin Appl Res*
891 **20**:11–21. doi:10.1016/j.jveb.2017.02.007

892 Runco MA, Charlop MH, Schreibman L. 1986. The occurrence of autistic children's self-
893 stimulation as a function of familiar versus unfamiliar stimulus conditions. *J Autism Dev*
894 *Disord* **16**:31–44. doi:10.1007/BF01531576

895 Schneider CA, Rasband WS, Eliceiri KW. 2012. NIH Image to ImageJ: 25 years of image
896 analysis. *Nat Methods* **9**:671–675. doi:10.1038/nmeth.2089

897 Shrout PE, Fleiss JL. 1979. Intraclass correlations: Uses in assessing rater reliability. *Psychol*
898 *Bull*. doi:10.1037/0033-2909.86.2.420

899 Stephenson-Jones M, Samuelsson E, Ericsson J, Robertson B, Grillner S. 2011. Evolutionary
900 conservation of the basal ganglia as a common vertebrate mechanism for action selection.
901 *Curr Biol* **21**:1081–1091. doi:10.1016/j.cub.2011.05.001

902 Strickler AG, Byerly MS, Jeffery WR. 2007. Lens gene expression analysis reveals

903 downregulation of the anti-apoptotic chaperone *alpha A-crystallin* during cavefish eye
904 degeneration. *Dev Genes Evol* **217**:771–782.
905 Timmermann M, Schlupp I, Plath M. 2004. Shoaling behaviour in a surface-dwelling and a cave-
906 dwelling population of a barb *Garra barreimiae* (Cyprinidae, Teleostei). *Acta Ethol* **7**:59–
907 64. doi:10.1007/s10211-004-0099-8
908 Van Trump WJ, Coombs S, Duncan K, McHenry MJ. 2010. Gentamicin is ototoxic to all hair
909 cells in the fish lateral line system. *Hear Res* **261**:42–50.
910 Vogel S. 1983. Life in moving fluids. New Jersey: Princeton University Press.
911 Wilkens H, Hecht Max K, Wallace Bruce, Wilkens H. 1988. Evolution and genetics of epigean
912 and cave Astyanax-fasciatus (Characidae, Pisces) - Support for the neutral mutation theory
913 In: Hecht M K, Wallace B, editors. Evolutionary Biology. New York: Plenum Publishing
914 Corporation. pp. 271–367. doi:10.1007/978-1-4613-1043-3_8
915 Wilson E V, Thomas RQ, Evans LM. 2004. Macrobrachium as a possible determinant of
916 *Astyanax fasciatus* distribution in a neotropical lowland stream. *Dartmouth Stud Trop Ecol*
917 **2004**:99–102.
918 Yoshizawa M. 2015. Behaviors of cavefish offer insight into developmental evolution. *Mol*
919 *Reprod Dev* **82**:268–280. doi:10.1002/mrd.22471
920 Yoshizawa M, Ashida G, Jeffery WR. 2012. Parental genetic effects in a cavefish adaptive
921 behavior explain disparity between nuclear and mitochondrial DNA. *Evolution (N Y)*
922 **66**:2975–2982. doi:10.1111/j.1558-5646.2012.01651.x
923 Yoshizawa M, Gorički S, Soares D, Jeffery WR. 2010. Evolution of a behavioral shift mediated
924 by superficial neuromasts helps cavefish find food in darkness. *Curr Biol* **20**:1631–1636.
925 doi:10.1016/j.cub.2010.07.017

926 Yoshizawa M, Settle A, Hermosura MCM, Tuttle LJL, Cetraro N, Passow CNCN, McGaugh
927 SESE. 2018. The Evolution of a Series of Behavioral Traits is associated with Autism-Risk
928 Genes in Cavefish. *BMC Evol Biol* **18**:89. doi:10.1186/s12862-018-1199-9
929
930

931 **Figure Legends**

932 **Figure 1. Schematics of the behavioural assay.**

933 (A) Schematics of the assay system. The recording tank was back-lighted by an infrared (IR)
934 LED array with a white paper diffuser. The IR camera was set at the top of the tank, and fish
935 movement was recorded. (B) One example frame of recorded cavefish video. Coloured lines
936 represent the 1-s (20 frames) trajectories of individual fish detected by idTracker software. (C)
937 Example trajectories of each cavefish from a 2.5-min recording. Each fish shape's ID was
938 determined by idTracker, and its X-Y coordinates were traced across the entire recording time.
939 The top row (4 panels) shows the X-Y-time traces of each of four fish. The bottom row
940 represents the X-Y traces by stacking the time series of the corresponding top row panel.

941

942 **Figure 2. Detection of social-like nearby interactions.**

943 (A, B) Measurements of nearest neighbour distance (NND) (A) and inter-individual distance
944 (IID) (B). Surface fish are shown as black lines, and cavefish are shown as orange lines (N= 18
945 groups of four, each). The means ± standard error of the mean (s.e.m.) at each frame are shown.
946 Insets show averages of NND or IID sampled every 30 s of the 300-s assays. n.s.: not significant.
947 (C) An example frame of recorded surface fish video. Coloured lines represent trajectories of
948 individual fish detected by idTracker software (1-s/20-frame trajectories). A red-labelled fish
949 was followed by a blue-labelled fish. (D) Distribution of IID across all frames of 18 surface fish
950 groups, where each group yields six IIDs from each pair among the 4 fish ($_4C_2 = 6$, black line:
951 means ± 95% confidence intervals (CIs)). Similarly, the distribution of IIDs was calculated from
952 1,280 simulated randomly sampled groups (blue line: means ± 95% CI). IID between 3 and 6 cm
953 showed significant separation between actual and simulated IIDs (yellow shaded areas). Inset

954 shows the magnified 3-6 cm interval. *: P < 0.05, *t*-test between the actual and simulated data
955 adjusted by the Holm correction within the yellow shaded area. (E) Inverse cumulative
956 distribution of the nearby-event durations. The inverse cumulative distributions for the event
957 durations whose IIDs were less than 5 cm are shown, where the black lines represent the results
958 from the actual 18 surface fish groups (means ± 95% CI) and the blue lines represent the results
959 of the 1,280 simulated groups (means ± 95% CI). In the actual surface fish data, the nearby-
960 interaction durations between 3 and 8 s were significantly higher than the simulated surface fish
961 data. **: P < 0.01, *t*-test between the actual and simulated data adjusted by the Holm correction
962 within the yellow shaded area. (F) Swimming velocity during or out of nearby interactions. The
963 mean swimming speeds (1) during the 4 s before the nearby-interaction bout, (2) during the bout,
964 (3) during 4 s after the bout, and (4) during out-of-bout periods are shown for surface fish (left)
965 and cavefish (right) by using the actual and simulated dataset (N=72 from 18 groups for each of
966 surface fish and cavefish and for each of the actual and randomly sampled data). Swimming
967 speeds are lower in the cavefish during the bout in the actual data. (G) Pirate plots depicting
968 nearby-interaction durations detected by the newly developed method. The plot of the actual data
969 is shown in black and white, and the simulated data are shown in light blue (N=72 from 18
970 groups for each of the surface fish and cavefish). The thicknesses of the beans represent data
971 density. *: P < 0.05, ***: P < 0.001. All statistical scores are available in Supplementary File 1.
972 The new detection protocol for determining nearby interactions is described in Supplementary
973 File 2 and Figure 2—figure supplements 1-3. The involvement of the lateral line sensory system
974 in the nearby interaction was tested, and the data are presented in Figure 2—figure supplement 4.
975

Figure 3. Reduced social-like nearby interactions in cavefish in unfamiliar environments compared with familiar environments.

(A) Schematics of experimental procedure. Fish were acclimated in the home tray for more than 4 days and were transferred to the recording tank in this unfamiliar environment. After the recording, fish were returned to the home tray where they remained for more than 4 days. Then, the fish were returned to the recording tank and acclimated to the recording tank for 4 days. After acclimation, an infrared (IR) LED array was set to illuminate fish, and fish movements were recorded in this familiar environment. (B) The position index to characterize location preference (top view of the recording arena). Region 1 represents the centre, and region 0 represents the peripheral area of the recording. The areas of both region 1 and 0 are exactly the same. (C) Plots for the positional preference of the fish for region 1. The longer bars at the middle of the beans represent medians, and shorter bars represent 25th (bottom bar) and 75th (top) percentiles. Positional preference showed no significant change between the familiar and unfamiliar environments, but surface fish preferred the peripheral area more than cavefish. (D) Swimming distance plots indicated that cavefish swam significantly longer distances than surface fish. Surface fish had lower swimming distances in the unfamiliar environment. (E) The turning bias index indicated that cavefish turned more unidirectionally than surface fish, and the environmental shift did not affect the turning bias. (F, G) The duration (F) and the number of nearby-interaction bouts: both scores supported a significantly higher level of nearby interactions in surface fish. Notably, the nearby-interactions durations (G) showed similar scores in the familiar environment between surface fish and cavefish, yet the unfamiliar stimulus increased (surface fish) or decreased (cavefish) the duration, resulting in a significant Env × Pop interaction in the generalized linear model (Supplementary File 1). (H) Swimming velocity

during or out-of-nearby interactions. The mean swimming speeds (1) during 4 s before the nearby-interaction bout, (2) during the bout, (3) during 4 s after the bout, and (4) during the out-of-bout period are plotted for surface fish (left) and cavefish (right) in the familiar and nonfamiliar environments. The average speed was reduced during the bout in cavefish under both familiar and unfamiliar environments. In contrast, the surface fish changed their speed profile only in the unfamiliar environment. SF: surface fish (N=36 from 9 groups); CF: cavefish (N=36 from 9 groups). **: $P < 0.01$, ***: $P < 0.001$. All detailed statistical scores are available in Supplementary File 1.

Figure 4. Turning bias index showed strong biased turning in cavefish.

(A) Diagram showing the calculation formula for the turning bias index. The changes in travelling directions were calculated every 5 frames (every 0.25 s) across all trajectories and were expressed as radians. Positive radian values represent left (anticlockwise) turning, and vice versa. Then, the $\log_2$ of the ratio between the numbers of clockwise and anticlockwise turns was used as the turning bias index. (B, C) Histograms of the turning bias index for 72 surface fish (B) and 72 cavefish (C) in the unfamiliar environment (see the main text). (D, E) Swimming trajectories representing a range of turning bias indices in surface fish (D) and cavefish (E). The replication test regarding turning bias in cavefish is shown in Figure 4—figure supplement 1. The source data for the histogram are available in Figure 4—source data 1.

Figure 5. The relationship between repetitive turning behaviour and nearby social-like behaviour in cavefish.

1021 (A, B) In the familiar environment, the logarithmic transformed turning bias index and aspects of
1022 nearby interactions were significantly negatively correlated, $F_{1,34} = 9.6$, adjusted $R^2 = 0.198$, P =
1023 0.0038 for the turning bias index against the nearby-interaction durations (A); $F_{1,34} = 10.0$,
1024 adjusted $R^2 = 0.204$, P = 0.0033 for the turning bias index against the number of nearby-
1025 interaction bouts (B). (C, D) In contrast, in the unfamiliar environment, aspects of the nearby
1026 interactions were reduced, and lower correlations were detected, $F_{1,34} = 3.6$, adjusted $R^2 = 0.069$,
1027 P = 0.0659 for the turning bias index against the nearby-interaction durations (C); $F_{1,34} = 4.6$,
1028 adjusted $R^2 = 0.094$, P = 0.0384 for the turning bias index against the number of nearby-
1029 interaction bouts (D). *: $P < 0.05$, **: $P < 0.01$. Red dashed lines: regression lines with the
1030 logarithmic transformation on the x-axis. Grey shades represent 95% confidence intervals of the
1031 regression lines (N = 36 from 9 groups).
1032
1033 **Figure 6. The partial agonist of the D2 receptor aripiprazole enhanced nearby interactions**
1034 **and reduced turning bias in cavefish.**
1035 The pre-treatment behaviours were recorded for more than four days before the aripiprazole
1036 treatment. Aripiprazole and the control DMSO were administered for ~16 hours before the post-
1037 treatment recording in an unfamiliar environment. (A) Total swimming distances before (black
1038 and white) and after (red shaded) the treatment, between the aripiprazole and control treatments,
1039 and between surface fish and cavefish. The cavefish had significantly reduced swimming
1040 distances after aripiprazole treatment. (B) The turning bias index indicated that cavefish
1041 significantly reduced biased turning after aripiprazole treatment. (C) The nearby-interaction
1042 durations showed a significant difference in Pop (surface fish and cavefish) and a significant
1043 interaction with PrePost (pre- and post-treatment) × Pop via a general linearized model

1044 (Supplementary File 1). Post hoc tests indicated a significant increase in nearby interactions in
1045 the aripiprazole-treated cavefish. (D) Significant difference in Pop (surface fish and cavefish).
1046 (E, F) Swimming speed during bouts or out-of-bout periods in surface fish (E) and cavefish (F).
1047 Aripiprazole treatment did not change the speed profiles in either the surface fish or cavefish.
1048 N=20 from 5 groups for surface fish control; N=16 from 4 groups for aripiprazole-treated surface
1049 fish; N=28 from 7 groups for cavefish control; N=32 from 8 groups for aripiprazole-treated
1050 cavefish. *: $P < 0.05$, **: $P < 0.01$, ***: $P < 0.001$. All statistical scores are available in
1051 Supplementary File 1. Regression plots between the nearby-interaction durations and swimming
1052 speeds are available in Figure 6–figure supplement 1.
1053
1054

1055 **List of Supplementary Files**

1056 **Figure Supplements**

1057 Figure 1—figure supplement 1. No visual response to the back light emitted from the 850-nm
1058 infrared (IR) LED.

1059 Figure 2—figure supplement 1. Determining the cut-off distance and cut-off duration for
1060 detecting nearby interactions.

1061 Figure 3—figure supplement 2. Determining cut-off durations for detecting nearby interactions.

1062 Figure 3—figure supplement 3. Fish traces of detected nearby interactions using different cut-off
1063 distances in surface fish.

1064 Figure 3—figure supplement 4. Fish traces of detected nearby interactions using different cut-off
1065 distances in cavefish.

1066 Figure 3—figure supplement 5. Pharmacological ablation of the lateral line by gentamicin
1067 antibiotics reduced nearby interactions.

1068 Figure 3—figure supplement 6. Shifts in swimming velocity during or out of nearby-interaction
1069 bouts.

1070 Figure 4—figure supplement 1. Replication test assessing turning bias in cavefish.

1071 Figure 6—figure supplement 1. Swimming speed is not a significant predictor of nearby-
1072 interaction durations.

1073

1074 **Videos**

1075 Video 1. Swimming patterns of four surface fish in dark conditions (unfamiliar environment).

1076 Video 2. Swimming patterns of four cavefish in dark conditions (unfamiliar environment).

1077 Video 3. Swimming patterns of four surface fish in dark conditions. The arena was illuminated

with infrared light. Fish did not respond to the visual stimulus—a moving object (unfamiliar environment).

Video 4. Swimming patterns of four surface fish in lighted conditions (unfamiliar environment).

Supplementary Files

Supplementary File 1. Detailed statistical scores for Figures 2, 3, and 6 and their figure supplements.

Supplementary File 2. Standardization method for nearby interactions in the dark.

Supplementary File 3. DASPMI staining of mechanosensory neuromasts.

Figure supplement

Figure legends

Figure 1—figure supplement 1. No visual response to the back light emitted from the 850-nm infrared (IR) LED.

(A) Top view of the recording arena. Half of the area was IR illuminated from the bottom, and the other half was not illuminated. The areas of these two regions were exactly the same. No probability difference between these two areas was detected in surface fish (B) and cavefish (C). These probability scores were at chance level (0.5). Values are the means ± 95% confidence intervals (N=4 groups, each).

Figure 2—figure supplement 1. Determine the cut-off distance and cut-off duration for detecting nearby interactions.

(A, B and D) An example of nearby-interaction profiles in surface fish (a four-fish group). (A) A histogram of inter-individual distance (IID; left) and raster plot for the nearby-interaction events

1102 (blue background with yellow bars)—each pair of IIDs under the cut-off distance: 5 cm or less
1103 (right). IIDs were calculated across all frames (6,000 frames = 5 min) from all 6 pairs ($_4C_2 = 6$
1104 pairs). Six columns in the raster plot represent six pairs of 4 fish (e.g., fish 1 vs fish 2, fish 1 vs
1105 fish 3, fish 1 vs fish 4, fish 2 vs fish 3, fish 2 vs fish 4, and fish 3 vs fish 4). (B) The histogram of
1106 the bout durations for a given cut-off distance (5 cm or less) (left) and the raster plot of the bouts
1107 filtered by the cut-off duration (4 s or more) (right). (C) The schematic explains the average
1108 passing-by duration (PbDur). PbDur was subtracted from the durations of each nearby-
1109 interaction event, which standardized the nearby-interaction durations based on the means of
1110 swimming distance in a group. Please also see Materials and Methods and Supplementary File 2.
1111 (D) Fish trajectories during nearby interactions detected using the ≤ 5 cm and ≥ 4 s criteria with
1112 surface fish.
1113 Different line colours represent the trajectories of each of four fish. The thick lines represent the
1114 two fish trajectories in the first second of the bout, followed by thin lines, indicating the
1115 following trajectories during the bout. The top panel shows all nearby interactions from the top
1116 view of the arena. Bottom panels show each nearby interaction from the top view. The X- and Y-
1117 axes indicate positions of fish, and annotations for each panel show which pair (*e.g.*, fish 1 vs
1118 fish 2 at the far left-second bottom panel), how long (*e.g.*, 3.8 s), and which time point (*e.g.*, at
1119 75.8 s = frame 1,516). (E-G) are shown for an example of cavefish data corresponding to figures
1120 A, B and D.
1121
1122 **Figure 2—figure supplement 2. Details of nearby interactions were obtained by classifying**
1123 **them into five categories.**
1124 (A) Vector set and their angles for classifying interactions between a fish pair. $F1_t$ and $F1_{t-1}$ are

the positions of fish 1 at times t and t-1, respectively. Similarly, the positions of fish 2 are expressed as $F2_t$ and $F2_{t-1}$. The angles were calculated across each frame of 6,000 frames (5 min). (B) Classifying the nearby interactions into five categories based on the angles between two fish; (1) turquoise: two fish disperse each other; (2) blue: two fish swim in inverse directions; (3) red: two fish gather together; (4) yellow: fish 1 leads; (5) orange: fish 2 leads. (C) A raster plot example of nearby interactions in a surface fish group (four fish), where the interactions of fish pairs are colour-coded as in (B). Each pair (each column) shows frequent switches of the leading fish. (D) Each nearby interaction from the top view. The thick lines represent the fish trajectories during the first second of the bout. The thin lines represent the fish trajectories during the remainder of the bout, as shown in Figure 2—figure supplement 1D and G. (E, F) Example plots for a cavefish group (four fish) presented as in (C) and (D), respectively. As seen with surface fish (C and D), each cavefish pair (each column) also showed switches of the leading fish (e.g., pair 1 vs 3 and pair 1 vs 4 in (E)).

Figure 2—figure supplement 3. Nearby interactions of surface fish in lighted conditions. (A) An example frame of recorded surface fish video. Coloured lines represent trajectories of each individual fish detected by idTracker software. Trajectories for 1 s (20 frames) are shown. (B) A histogram for the bout durations filtered by the cut-off distance (5 cm or less) in a 15-s recording (surface fish group: N =4). (C) A raster plot of the nearby-interaction bouts filtered by ≤ 5 cm and ≥ 4 s. The interaction categories for a fish pair are the same in Figure 2—figure supplement 2B. Frequent changes in the leading fish appeared within each pair and within each bout (i.e., frequent switches between orange (fish 1 leading) and yellow colours (fish 2 leading)). (D) Each nearby interaction from the top view. The thick lines represent the fish trajectories

1148 during the first second of the bout. The thin lines represent the fish trajectories during the
1149 remainder of the bout, as shown in Figure 2—figure supplement 1D and G.
1150
1151 **Figure 2—figure supplement 4. Pharmacological ablation of the lateral line by gentamicin**
1152 **antibiotics reduced nearby interactions.**
1153 Fish were bath-treated with 0.002% gentamicin for approximately 16 hours before the
1154 behavioural assay in an unfamiliar environment. The bath treatment was performed in home
1155 trays (15.6 × 15.6 × 5.7 cm Ziplock containers). Then, fish behaviours were recorded on the
1156 recording tray without gentamicin. The control treatment was performed with 1/1,000 × diluted
1157 phosphate buffered saline, which was gentamicin's solvent. (A) The nearby-interaction durations
1158 indicated a significant difference between populations and treatments. Post hoc tests indicated a
1159 significant decrease in nearby interactions in the gentamicin-treated groups of surface fish. (B-E)
1160 The neuromasts, units of the mechanosensory lateral line system, were visualized with DASPMI
1161 vital dye (green dots; Supplementary File 3) after the behavioural assay. DASPMI is
1162 incorporated into the mitochondrial cell membrane of functional hair cells and emits fluorescein;
1163 therefore, it labels only active neuromasts with functional hair cells (Jørgensen, 1989).
1164 Accordingly, there were many functional neuromasts following control treatment (B, D), and
1165 gentamicin-treated fish lost most of the stained (functional) neuromasts (C, E). N = 20 for
1166 control surface fish from 5 groups; N=24 for gentamicin surface fish from 6 groups; N=24 for
1167 control cavefish from 6 groups; and N=24 for gentamicin cavefish from 6 groups. *: $P < 0.05$,
1168 ***: $P < 0.001$. All statistical scores are available in Supplementary File 1.
1169
1170

1171 **Figure 4—figure supplement 1. Replication test assessing turning bias in cavefish.**

1172 (A) Each cavefish was first subjected to the turning assay in the individual recording arena to
1173 track their ID. After the initial recording, each cavefish was tattooed with visible implant
1174 elastomer according to the manufacturer's instructions under anaesthesia and then recovered in
1175 the home tray. Note that the elastomer tag was not visible in the video, and the cavefish appeared
1176 similar to each other. Then, 10 days after the initial recording, fish movements were recorded
1177 again. (B) Scatterplot of turning bias on the two different days. The individual fish that showed a
1178 strong left-turning bias consistently showed the same tendency 10 days later, and vice versa.
1179 Interclass correlation: kappa = 0.92, P = 0.0016, N = 6: the test-retest based on the two-way
1180 random effect models and "single rater" unit.

1181

1182 **Figure 6—figure supplement 1. Swimming speed is not a significant predictor of nearby-**
1183 **interaction durations.**

1184 Swimming speeds and nearby-interaction durations before (A) and after (B) treatment with
1185 aripiprazole (N=32 from 8 groups: $F_{1,18} = 2.1$, P = 0.1622; and $F_{1,18} = 0.1$, P = 0.8081,
1186 respectively) were not significantly correlated in cavefish. Similarly, those of surface fish were
1187 not correlated (C, D) (N=16 from 4 groups: $F_{1,14} = 0.4$, P = 0.5199; and $F_{1,14} = 4.3$, P = 0.0565,
1188 respectively). Red dashed lines: regression lines with the logarithmic transformation on the x-
1189 axis. Grey shades represent 95% confidence intervals of the regression lines.

1190

Figure 1

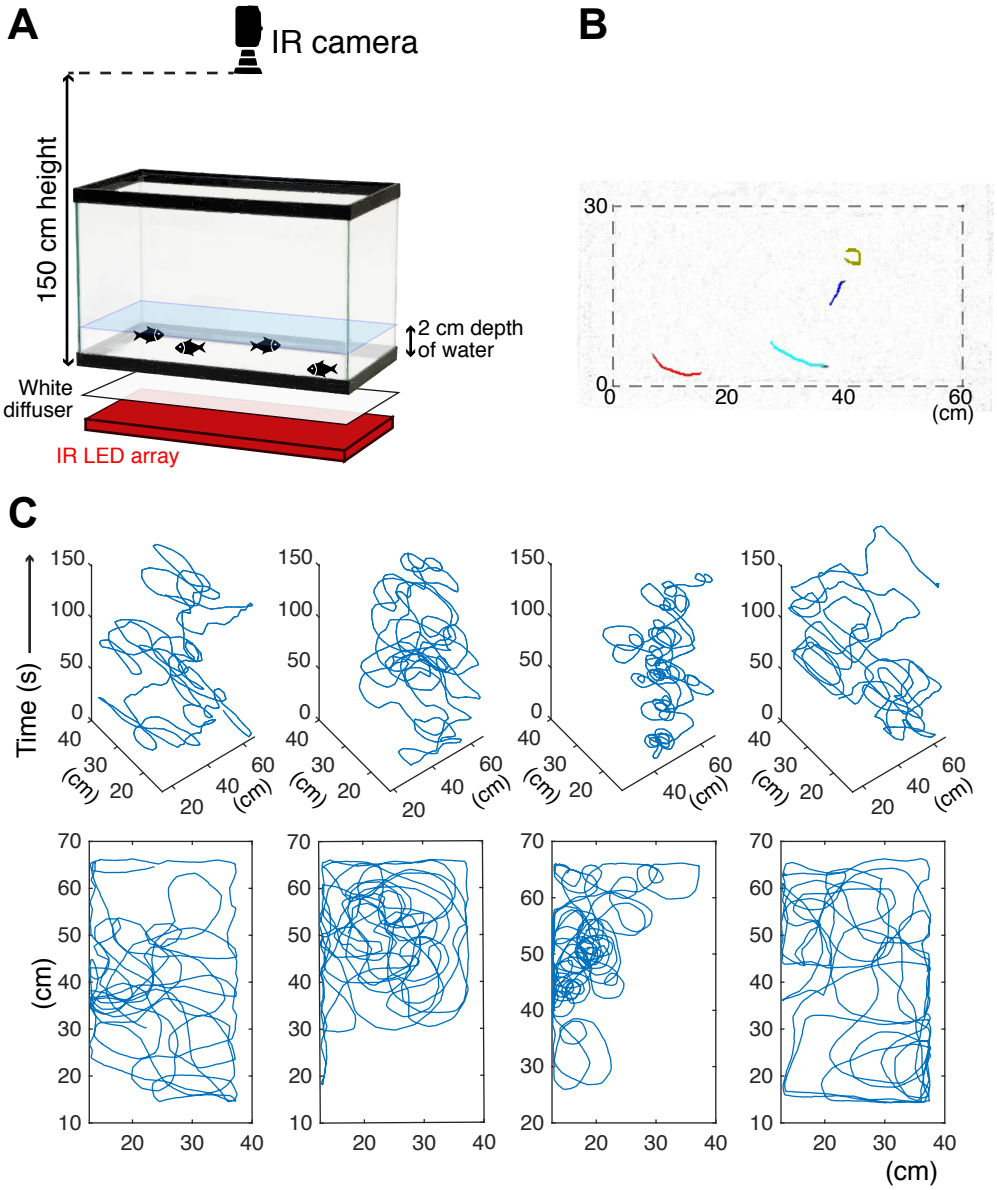
A
IR camera
150 cm height
2 cm depth
of water
White
diffuser
IR LED array
B
30
0
0
20
40
60
(cm)
C
Time (s)
150
100
50
0
40
30
20
(cm)
20
40
60
(cm)
70
60
50
40
30
20
10
(cm)
20
30
40
(cm)

Figure 1--figure supplement 1

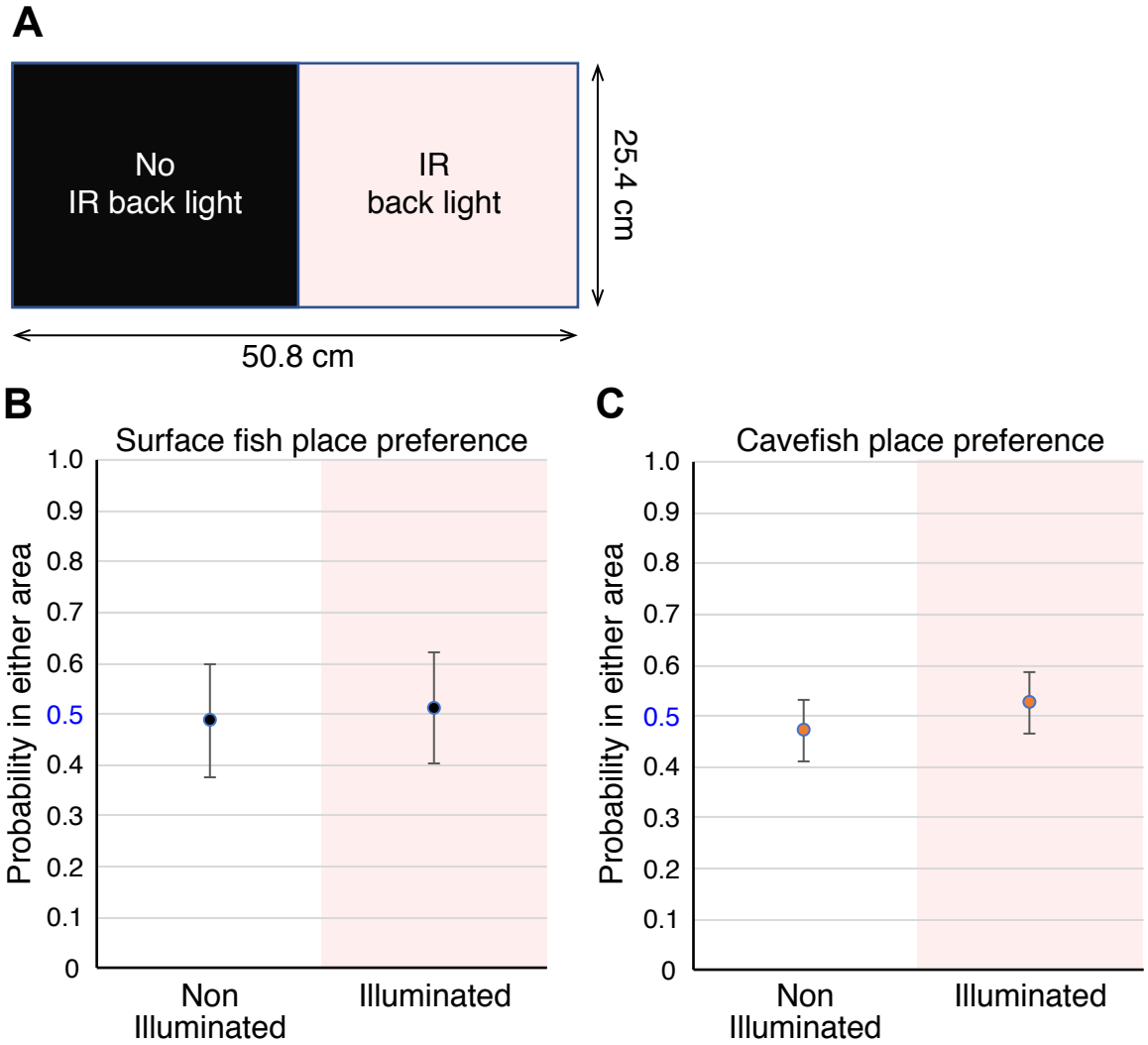

Figure 2

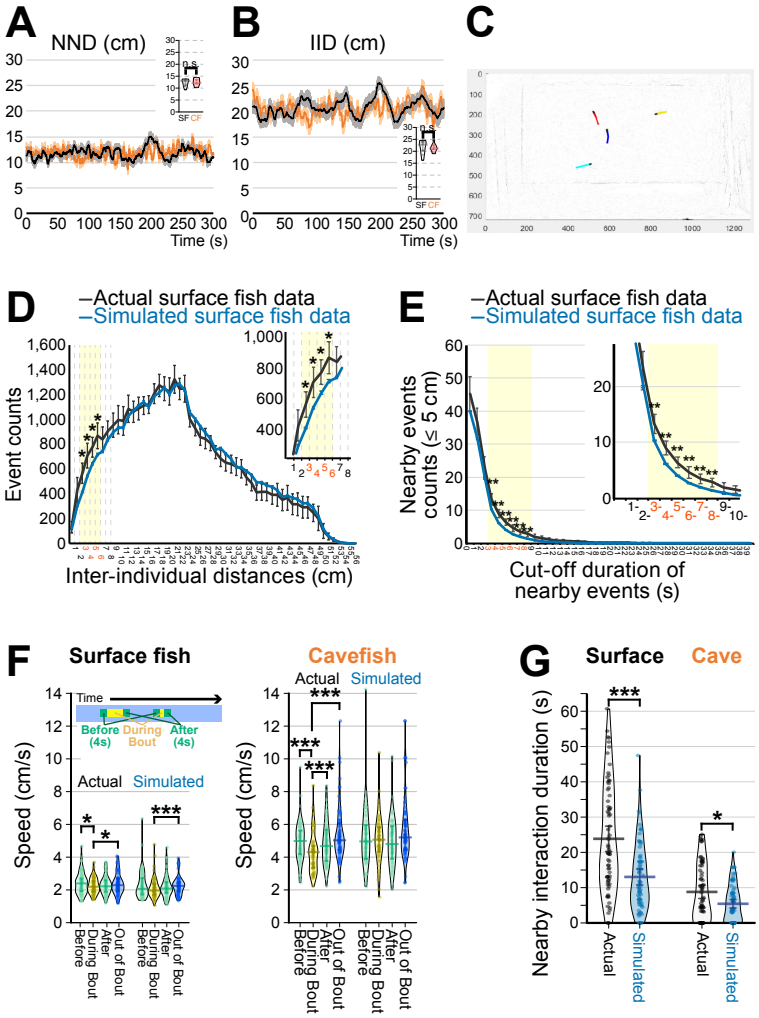
A
NND (cm)
Time (s)
B
IID (cm)
Time (s)
C
D
–Actual surface fish data
–Simulated surface fish data
Event counts
Inter-individual distances (cm)
E
–Actual surface fish data
–Simulated surface fish data
Nearby events counts (≤ 5 cm)
Cut-off duration of nearby events (s)
F
Surface fish
Cavefish
Time
Before (4s)
During Bout
After (4s)
Actual
Simulated
Speed (cm/s)
Before
During Bout
After
Out of Bout
G
Surface
Cave
Nearby interaction duration (s)
Actual
Simulated

Figure 2--figure supplement 1

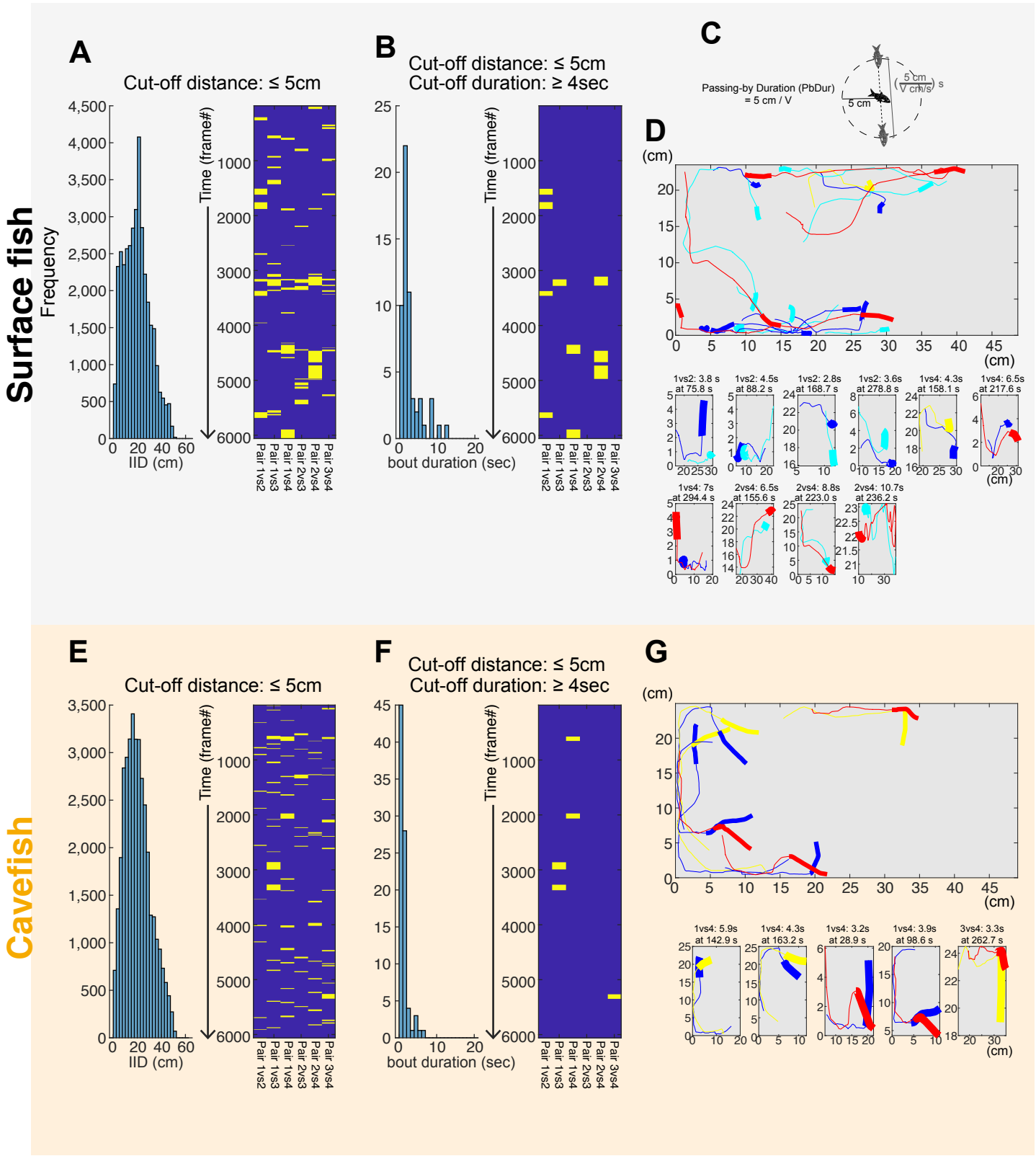

Figure 2--figure supplement 2

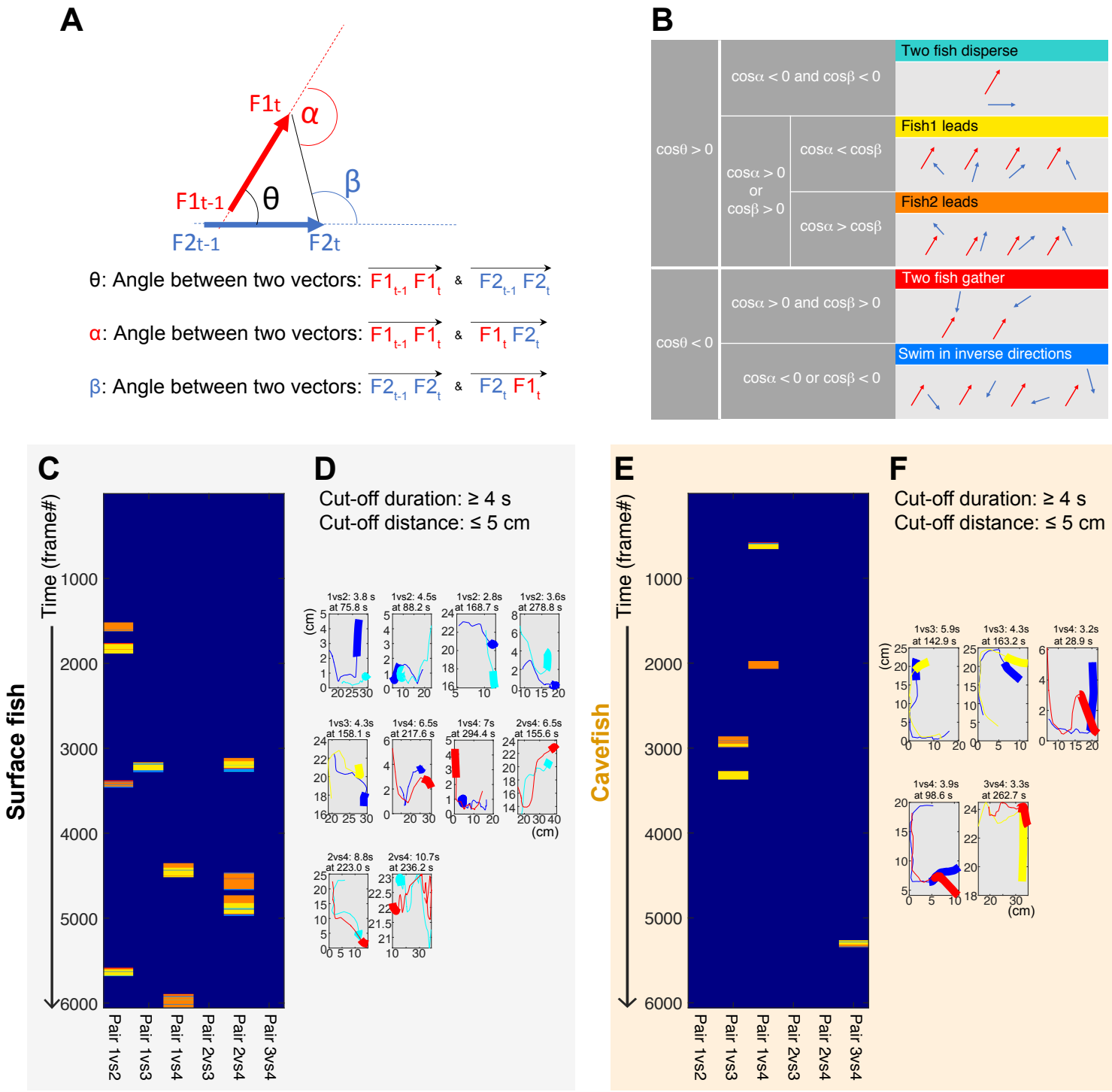

Figure 2--figure supplement 3

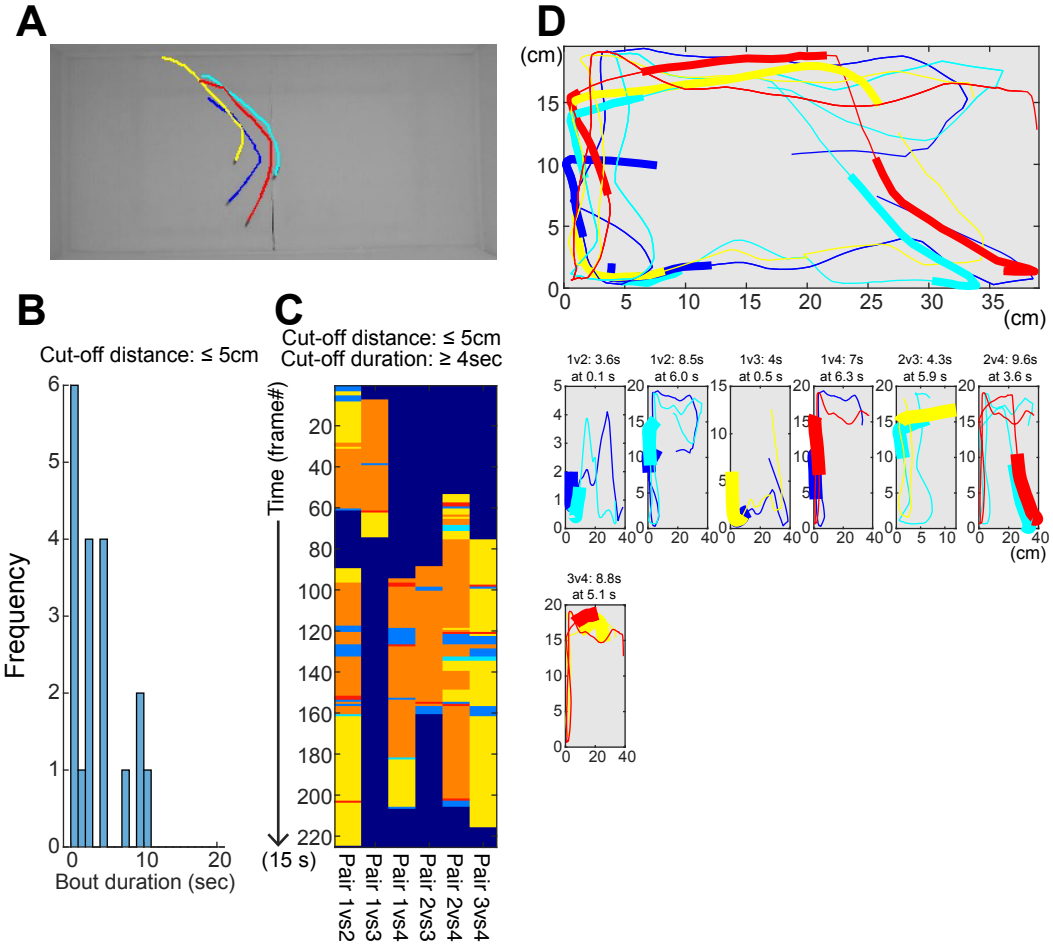

Figure 2--figure supplement 4

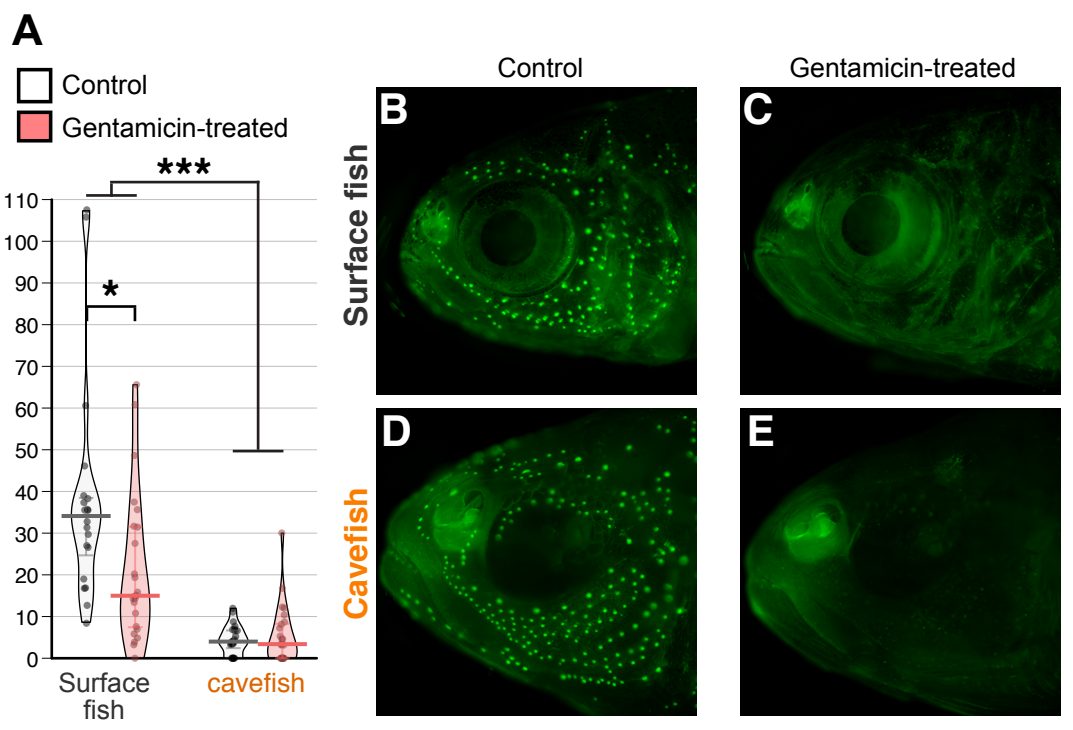

Figure 3

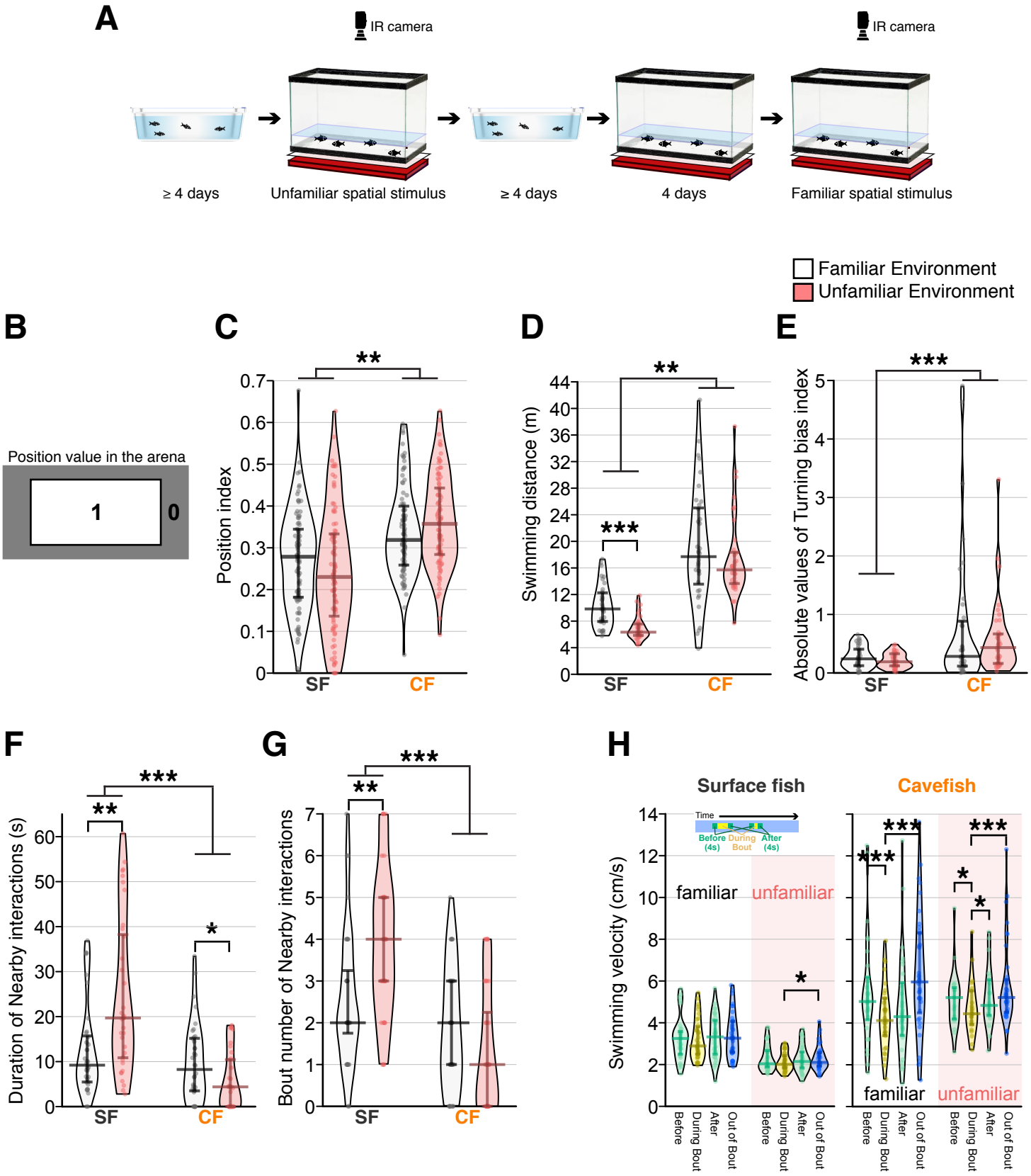
A
IR camera
IR camera
≥ 4 days
Unfamiliar spatial stimulus
≥ 4 days
4 days
Familiar spatial stimulus
Familiar Environment
Unfamiliar Environment
B
Position value in the arena
1
0
C
Position index
SF
CF
D
Swimming distance (m)
SF
CF
E
Absolute values of Turning bias index
SF
CF
F
Duration of Nearby interactions (s)
SF
CF
G
Bout number of Nearby interactions
SF
CF
H
Surface fish
Cavefish
Time
Before (4s)
During Bout
After (4s)
Swimming velocity (cm/s)
familiar
unfamiliar
familiar
unfamiliar
Before
During Bout
After
Out of Bout

Figure 4

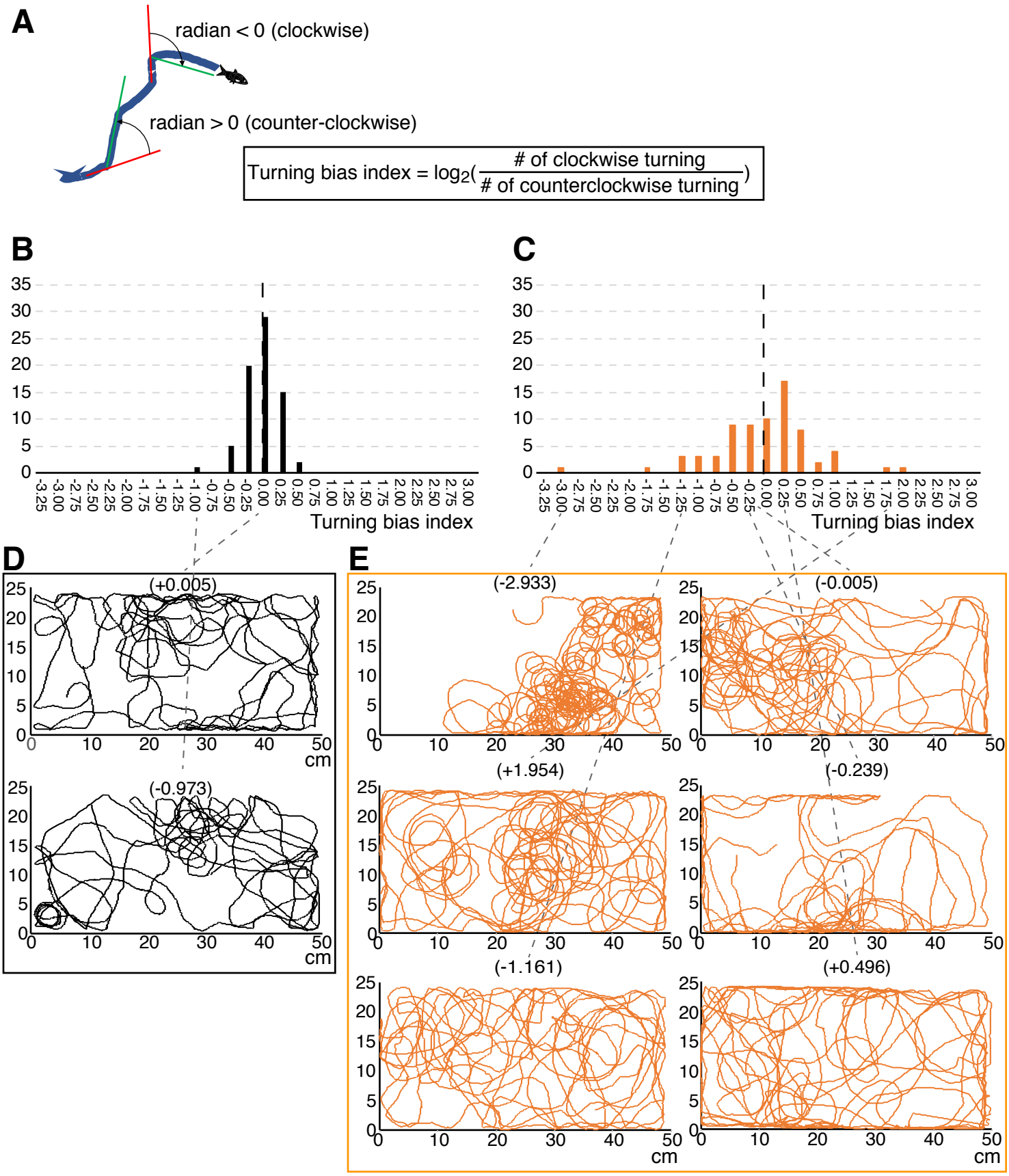
A
radian < 0 (clockwise)
radian > 0 (counter-clockwise)
Turning bias index = log2(# of clockwise turning / # of counterclockwise turning)
B
Turning bias index
C
Turning bias index
D
(+0.005)
(-0.973)
cm
E
(-2.933)
(-0.005)
(+1.954)
(-0.239)
(-1.161)
(+0.496)
cm

Figure 4--figure supplement 1

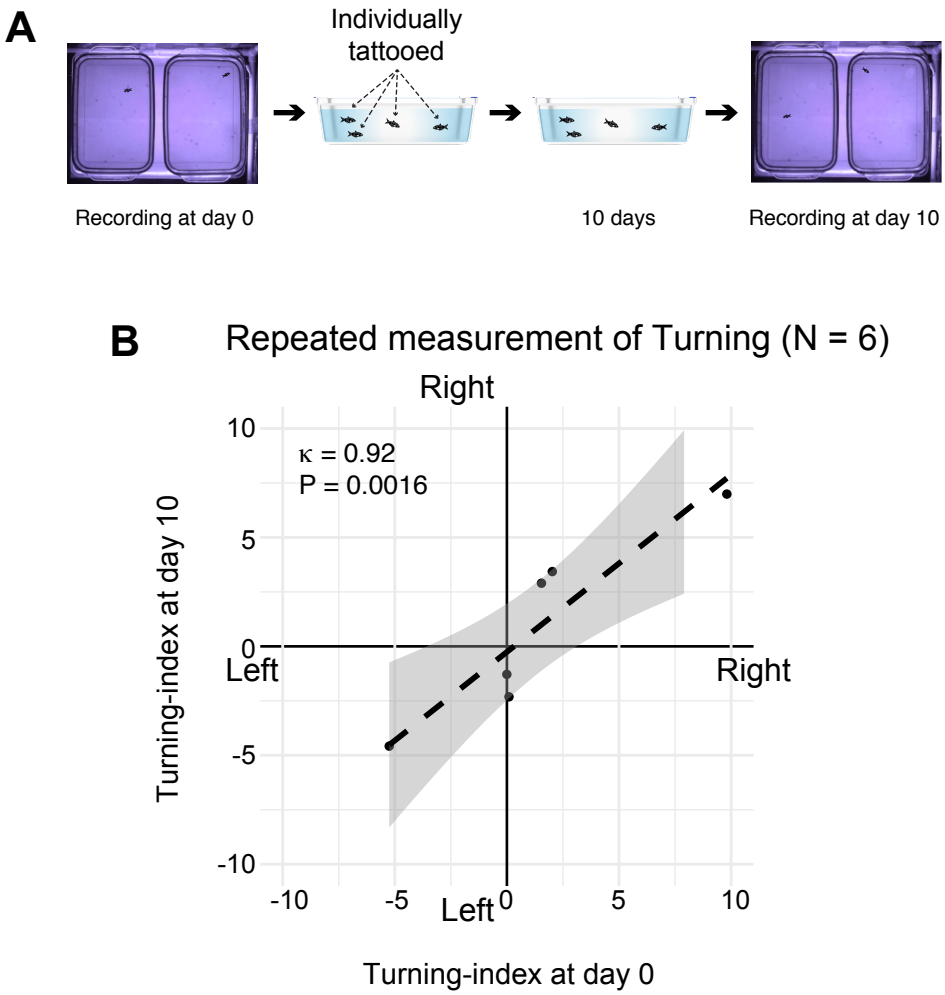

Figure 5

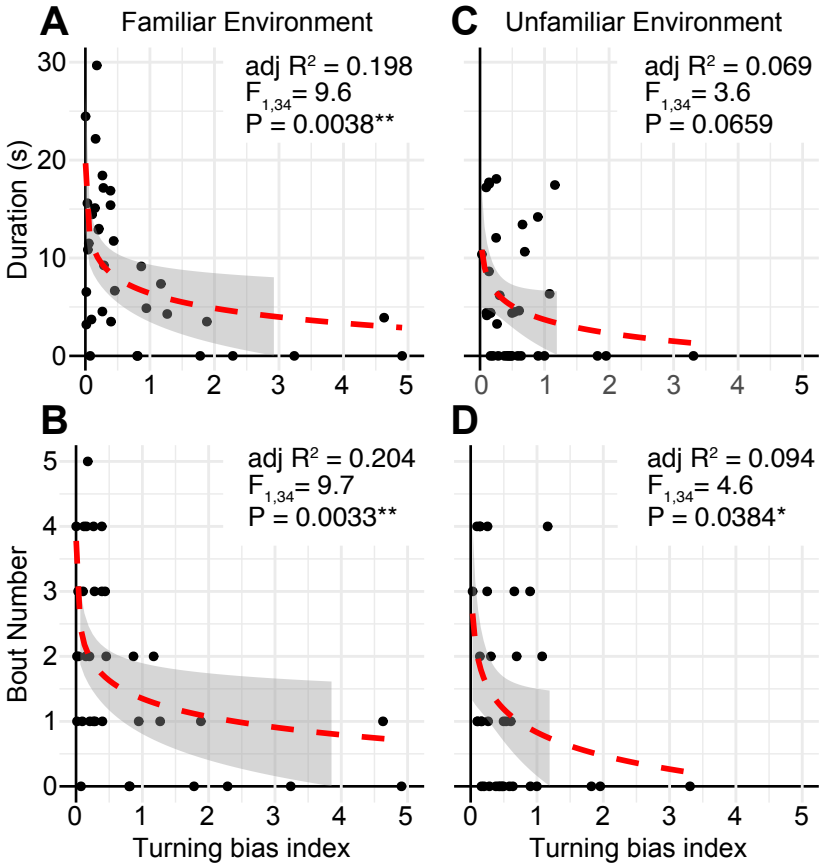
A
Familiar Environment
adj R² = 0.198
F1,34 = 9.6
P = 0.0038**
C
Unfamiliar Environment
adj R² = 0.069
F1,34 = 3.6
P = 0.0659
B
adj R² = 0.204
F1,34 = 9.7
P = 0.0033**
D
adj R² = 0.094
F1,34 = 4.6
P = 0.0384*
Duration (s)
Bout Number
Turning bias index
Turning bias index

Figure 6

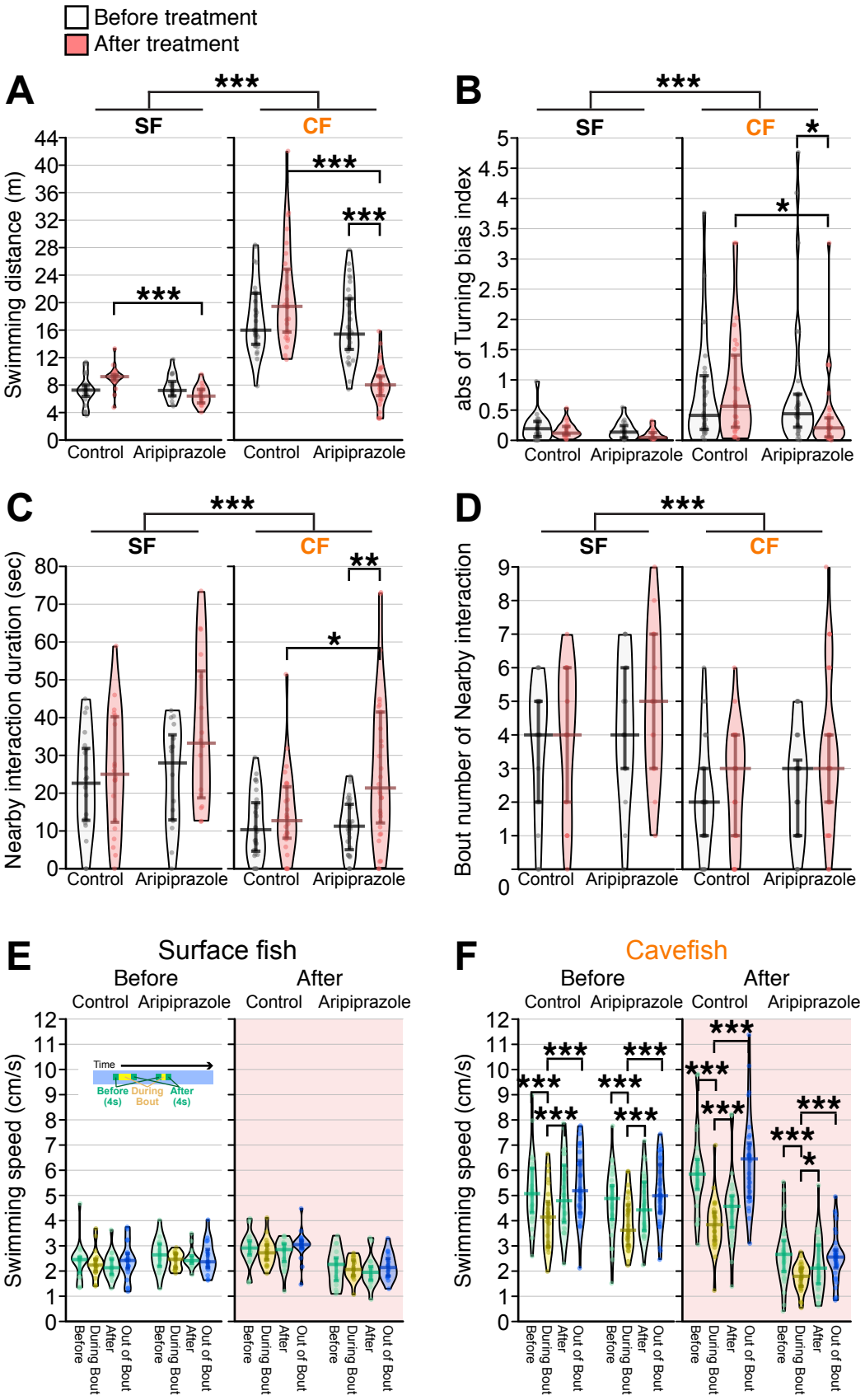
Before treatment
After treatment
A
B
C
D
E
F
SF
CF
Swimming distance (m)
abs of Turning bias index
Nearby interaction duration (sec)
Bout number of Nearby interaction
Control
Aripiprazole
Surface fish
Cavefish
Before
After
Swimming speed (cm/s)
Time
Before (4s)
During Bout
After (4s)
Out of Bout

Figure 6--figure supplement 1

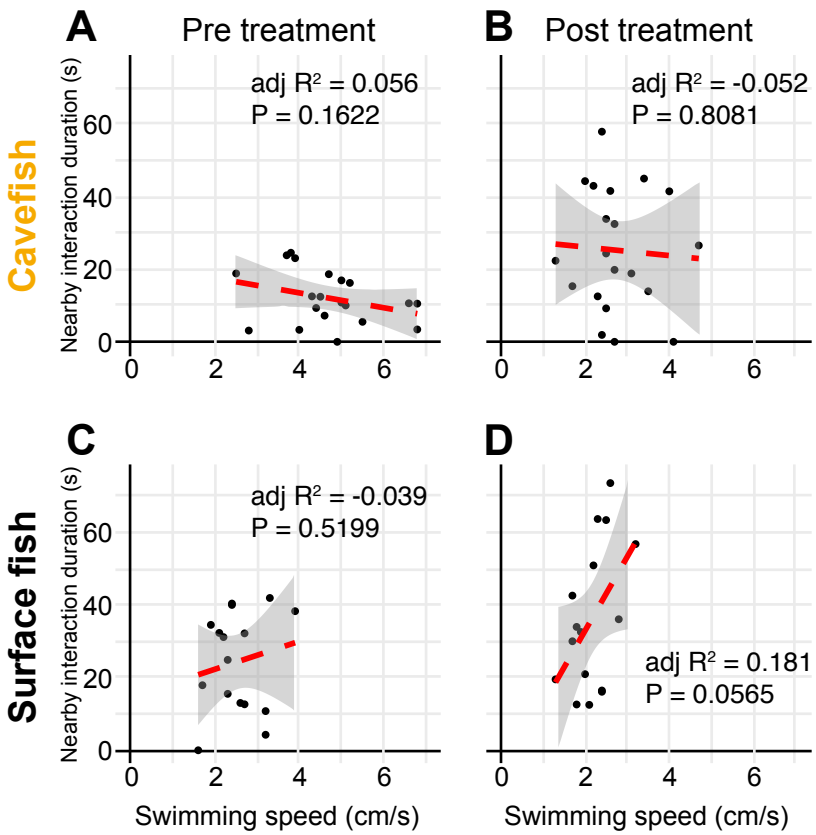

Supplementary File 2.
Standardization method for nearby interaction in the dark

To characterize social-like interactions, we developed an assay system incorporating a naturalistic free swimming set up that also deprived the fish of visual stimulus (See body text too). In previous reports, teleost fish display a wide array of collective behaviors (e.g., schooling and shoaling)(Pitcher and Parrish, 1993). Attempts have been made to quantitatively assay social interactions in some marine (sea beam, salmon) and a few freshwater teleost (cave barb and cave molly and their surface species/populations), revealing the major involvement of visual- and mechanosensing in teleost collective behavior (Bleckmann, 1986; Paciorek and Mcrobert, 2012; Pitcher, 1993; Pitcher and Parrish, 1993; Timmermann et al., 2004). However, the majority of these reports measured shoaling activity under light conditions (thus under visual stimuli) and by using two-choice setup where a social-target fish was constrained in a small compartment and let the focal fish approach the nearby area for the target fish (Gerlai, 2014). The 'constrained' setup is comparable to the popular three-chamber test used in mice to assay sociability and social novelty (Silverman et al., 2010). However, this spatial restriction is an unusual stimulus to fish, and does not allow the same pattern of water fluctuation/vortices to form as when fish swim freely, which significantly limits the ability of a focal fish to follow another by using lateral line mechanosensors (Bleckmann et al., 1991; McHenry and Liao, 2013). The lighted condition also promoted tighter shoaling in surface fish yet no detectable change in cavefish of *A. mexicanus* (Kowalko et al., 2013; Patch et al., 2020; Pierre et al., 2020). Our free-swimming setup is to address nearby interaction with an aid of idTracker auto-tracking software (Pérez-Escudero et al., 2014). Under our free-swimming assay system, sighted surface fish tightly shoaled/schooled under lighted condition as reported (Video 3) (Keene et al., 2016; Kowalko et al., 2013; Patch et al., 2020; Pierre et al., 2020).

According to how the nearby interactions happened more than chance, we set cut-off distance and duration of nearby interaction as ≤ 5 cm and ≥ 4 sec, respectively (see main text). We also standardized the social bouts with the passing-by duration (PbDur). PbDur is defined here as the average duration of a fish passing-by another fish where these fish do not express the nearby interaction. In order to remove the period that resulted from just physical proximity rather than the actual social-like interaction (been 'attracted'), the PbDur were subtracted from each bout of the nearby interaction durations. Derivation of PbDur as follows.

The average duration of passing-by within each 4-fish group (PbDur) was calculated from the average relative swimming velocity (V_r) and average traveling distance within 6 cm radius of another fish (Distance).
V_r is calculated based on the scenario that two nearby fish are swimming in the velocity of V—an average velocity of four fish in the same group (Materials and Methods and Figure 2 —figure supplement 1C). Given two fish swim in the velocity of $V_1 = V_2 = V$ (see below box), the relative velocity is:

$$|V_r| = 2 \cdot |V| \cdot sin\left(\frac{\theta}{2}\right). \quad \text{(eq. 1, see below box)}$$

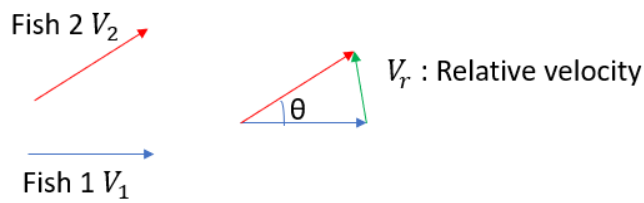

Fish 1 and Fish 2 are swimming in velocities of V_1 and V_2, respectively. Then, to simplify the calculation, suppose that the two fish swim with the average velocity, $V = V_1 = V_2$, the average of the relative velocity between two fish is given by V and θ (see above).

Then the average speed of V_r is:

$$E(|V_r|) = p(\theta) \cdot \int_0^{\pi} 2 \cdot |V| \cdot sin\left(\frac{\theta}{2}\right) d\theta \quad \text{(eq. 2)}$$

, where $p(\theta)$ is the uniform probability density distribution between 0 and π and expressed as:

$$p(\theta) = \frac{1}{\pi - 0} = \frac{1}{\pi} \quad \text{(eq. 3)}$$

Therefore, the average relative velocity becomes:

$$E(|V_r|) = \frac{1}{\pi} \cdot 2 \cdot |V| \cdot 2 = |V| \cdot \frac{4}{\pi} \quad \text{(eq. 4)}$$

Next, we calculated the average of traveling distances within a 5 cm radius of another fish.

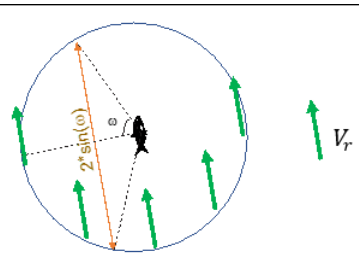

By using relative velocity, we can think as that one fish of a pair is still. Then, while another fish passing by a 5 cm radius of the first fish (circle), this fish travels 5 × 2 × $sin(\omega)$ cm (orange arrow).

With above assumption, the average of traveling distance L is then:

$$E(|L|) = 5\ (cm) \cdot p(\omega) \cdot \int_0^{\pi} 2 \cdot sin(\omega)\, d\omega \quad \text{(eq. 5)}$$

,where

$$p(\omega) = \frac{1}{\pi - 0} = \frac{1}{\pi} \quad \text{(eq. 6; see eq. 3 too)}$$

Therefore, the average traveling distance within a 5 cm radius is:

$$E(|L|) = 5\ (cm) \cdot \frac{1}{\pi} \cdot 2 \cdot 2 = 5\ (cm) \cdot \frac{4}{\pi} \qquad \text{(eq. 7)}$$

From $E(|V_r|)$ and $E(|L|)$ (eq. 4 and 7, respectively), the average passing-by duration (PbDur) is:

$$\text{PbDur} = \frac{E(|L|)}{E(|V_r|)} = \frac{5\ (cm) \cdot \frac{4}{\pi}}{|V| \cdot \frac{4}{\pi}} = \frac{5\ (cm)}{|V|} \qquad \text{(see Materials and Methods)}$$

References:

Bleckmann H. 1986. Role of the Lateral Line in Fish Behaviour In: Pitcher TJ, editor. The Behaviour of Teleost Fishes. London: Chapman & Hall. pp. 177–202. doi:10.1007/978-1-4684-8261-4_7

Bleckmann H, Breithaupt T, Blickhan R, Tautz J. 1991. The time course and frequency content of hydrodynamic events caused by moving fish, frogs, and crustaceans. *J Comp Physiol, A* **168**:749–757.

Gerlai R. 2014. Social behavior of zebrafish: From synthetic images to biological mechanisms of shoaling. *J Neurosci Methods* **234**:59–65. doi:10.1016/j.jneumeth.2014.04.028

Keene AC, Yoshizawa M, McGaugh SE. 2016. Biology and Evolution of the Mexican Cavefish, Biology and Evolution of the Mexican Cavefish. Amsterdam: Elsevier Inc. doi:10.1016/C2014-0-01426-8

Kowalko JE, Rohner N, Rompani SB, Peterson BK, Linden TA, Yoshizawa M, Kay EH, Weber J, Hoekstra HE, Jeffery WR, Borowsky R, Tabin CJ. 2013. Loss of schooling behavior in cavefish through sight-dependent and sight-independent mechanisms. *Curr Biol* **23**:1874–83. doi:10.1016/j.cub.2013.07.056

McHenry MJ, Liao JC. 2013. The Hydrodynamics of Flow StimuliThe Lateral Line System. Springer Handbook of Auditory Research 48. New York: Springer. pp. 73–98. doi:10.1007/2506_2013_13

Paciorek T, Mcrobert S. 2012. Daily variation in the shoaling behavior of zebrafish Danio rerio. *Curr Zool* **58**:129–137. doi:10.1093/czoolo/58.1.129

Patch A, Paz A, Holt K, Duboue E, Kowalko J, Keene A, Fily Y. 2020. Analysis of social swimming dynamics in the Mexican cavefish. *bioRxiv* 2020.01.31.929323. doi:10.1101/2020.01.31.929323

Pérez-Escudero A, Vicente-Page J, Hinz RC, Arganda S, De Polavieja GG. 2014. IdTracker: Tracking individuals in a group by automatic identification of unmarked animals. *Nat Methods* **11**:743–748. doi:10.1038/nmeth.2994

Pierre C, Pradère N, Froc C, Ornelas-García P, Callebert J, Rétaux S. 2020. A mutation in monoamine oxidase (MAO) affects the evolution of stress behavior in the blind cavefish Astyanax mexicanus. *bioRxiv* 2020.04.09.033266. doi:10.1101/2020.04.09.033266

Pitcher TJ. 1993. Behaviour of teleost fishes, Second. ed, Behaviour of Teleost Fishes. London: Chapman & Hall. doi:10.1007/978-1-4684-8261-4

Pitcher TJ, Parrish JK. 1993. Functions of Shoaling Behaviour in Teleosts In: Pitcher TJ, editor. Behaviour of Teleost Fishes. London: Chapman & Hall. pp. 363–440. doi:10.1007/978-1-

4684-8261-4_12
Silverman JL, Yang M, Lord C, Crawley JN. 2010. Behavioural phenotyping assays for mouse models of autism. *Nat Rev Neurosci* **11**:490–502. doi:10.1038/nrn2851
Timmermann M, Schlupp I, Plath M. 2004. Shoaling behaviour in a surface-dwelling and a cave-dwelling population of a barb *Garra barreimiae* (Cyprinidae, Teleostei). *Acta Ethol* **7**:59–64. doi:10.1007/s10211-004-0099-8

Supplementary File 3.
DASPMI staining of mechanosensory neuromasts

Neuromast vital staining was performed as described previously (Fernandes et al., 2018; Jørgenson, 1989; Worsham et al., 2019; Yoshizawa et al., 2010). Within 30 min after the video recording, each tested fish was isolated into a 100 ml beaker and immersed in 2.5 µg/ml 4-(4-(dimethylaminostyryl)-1-methylpyridinium iodide (4-Di-1-ASP or DASPMI; MilliporeSigma, Burlington, MA) dissolved in conditioned water for 30 min to one hour, followed by anesthesia in ice-cold 66.7 µg/mml Ethyl 3-aminobenzoate methanesulfonate salt (MS-222, MilliporeSigma) in conditioned water. Fish were then visualized under the fluorescence microscope (BX61WI Olympus microscope with 2.5 x MPlanFL N lens, a Rhodamine filter set and an ORCA-Flash4.0 digital camera). After the imaging, fish were recovered in the conditioned water at approx. 22 ˚C.

<u>Gentamicin treatment to ablate the lateral line neuromasts</u>
For the gentamicin treatment, gentamicin was bath treated as described (Yoshizawa et al., 2010). Briefly, a 0.002% solution of gentamicin sulfate salt (MilliporeSigma) in conditioned water was prepared and treated for 16–18 hrs prior to the experiment. The fish behaviors were assayed as described in the "Recording group fish behavior" without gentamicin, and analyzed as described in the "Tracking" subsections in the Materials and Method section.

References:
Fernandes VFL, Macaspac C, Lu L, Yoshizawa M. 2018. Evolution of the developmental plasticity and a coupling between left mechanosensory neuromasts and an adaptive foraging behavior. *Dev Biol* **441**:262–271. doi:10.1016/j.ydbio.2018.05.012

Jørgenson JM. 1989. Evolution of octavolateralis sensory cells In: Coombs S, Görner P, Münz H, editors. The Mechanosensory Lateral Line. New York: Springer-Verlag. pp. 115–145.

Worsham M, Lima Fernandes VF, Settle A, Balaan C, Lactaoen K, Tuttle LJ, Iwashita M, Yoshizawa M. 2019. Behavioral tracking and neuromast imaging of Mexican cavefish. *J Vis Exp* **2019**. doi:10.3791/59099

Yoshizawa M, Gorički S, Soares D, Jeffery WR. 2010. Evolution of a behavioral shift mediated by superficial neuromasts helps cavefish find food in darkness. *Curr Biol* **20**:1631–1636. doi:10.1016/j.cub.2010.07.017